Behavior of BCC metals under extreme conditions

Literature Review

Gaia Righi

April 21, 2020

Committee:
Dr. Marc A. Meyers (chair)
Dr. Anne Pommier
Dr. Farhat Beg
Dr. Nicholas Boechler
Dr. Javier Garay

UC San Diego

Overview of presentation

Background

Low $\dot{\varepsilon}$

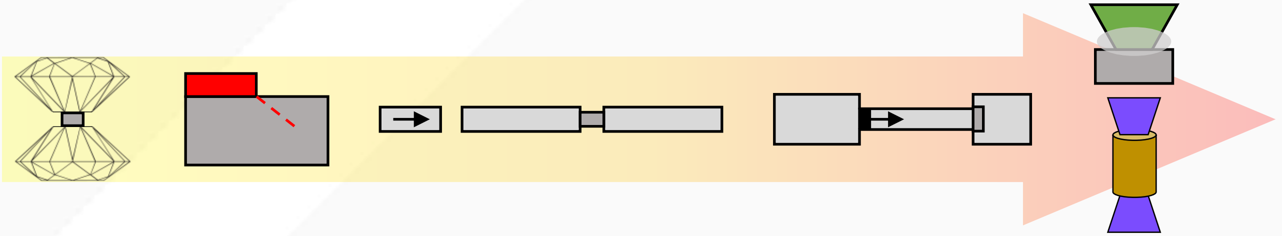

High $\dot{\varepsilon}$

Materials of Interest

74 **W** | 42 **Mo** | 23 **V** | 73 **Ta** | 26 **Fe**

Research Direction

26 **Fe**

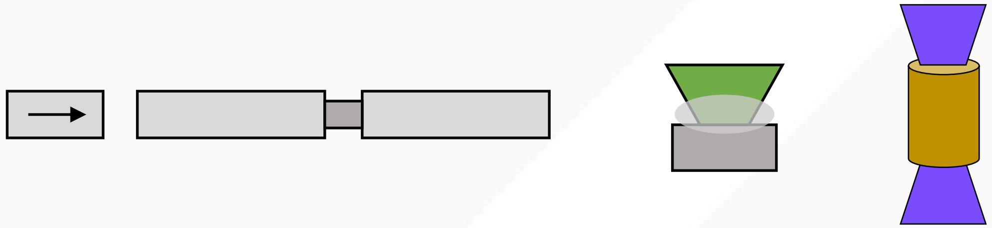

What are Extreme Conditions?

- Pressure ~ 1000 GPa
- Strain rates > $10^6\ s^{-1}$
- High temperatures
- Radiative environments
- Corrosive environments

APPLICATIONS

TRADITIONAL AND NOVEL ARMOR AND ANTI-ARMOR CONCEPTS
ADVANCED COMPUTATIONAL METHODS FOR DYNAMIC EVENTS
HIGH-STRENGTH, LIGHT-WEIGHT, IMPACT-RESISTANT MATERIALS
IMPACT CRATERING
HIGH-SPEED FABRICATION PROCESSES
NOVEL NDE METHODS
STUDY OF PLANETARY INTERIORS
PREDICTION OF EARTHQUAKE RESPONSE
CRASHWORTHINESS
SHIELDING FOR SPACE VEHICLES
EXPLOSIVE WELDING, FORMING, COMPACTION

Meyers, M.A., 1994. Dynamic Behavior of Materials, J. Wiley.

Extreme Conditions can be achieved via both static and dynamic methods.

Static (low $\dot{\epsilon}$)

Multi Anvil Apparatus

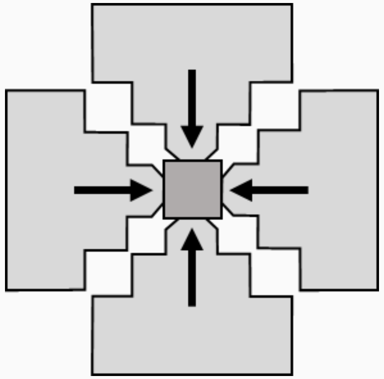

Diamond Anvil Cell

$$\dot{\epsilon} = 10^{-3} - 10^{-1}s^{-1}$$

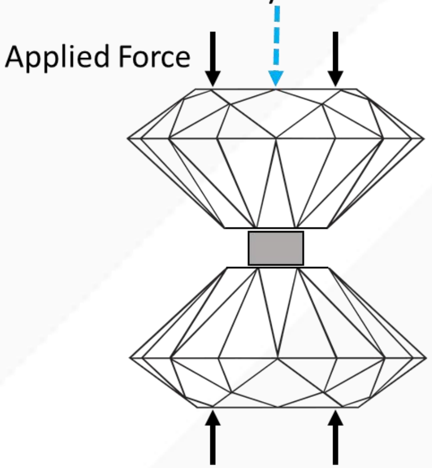

Dynamic (high $\dot{\epsilon}$)

Explosive devices

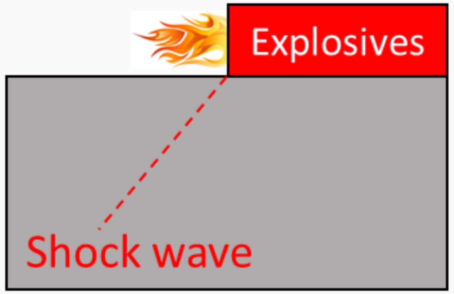

$$\dot{\epsilon} = < 10^{4}s^{-1}$$

Hopkinson Bar

$$\dot{\epsilon} = 10^{2} - 10^{4}s^{-1}$$

Gas Gun

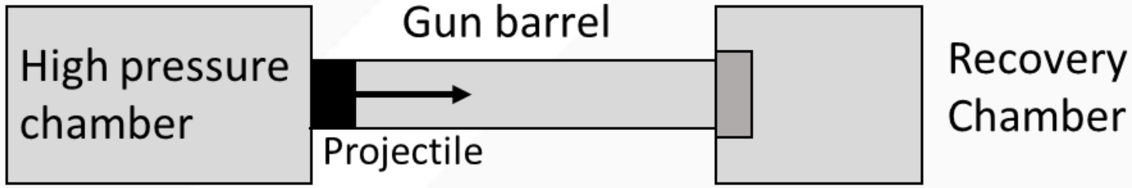

Laser shock is a dynamic method to achieve largest pressures and strain rates.

Direct

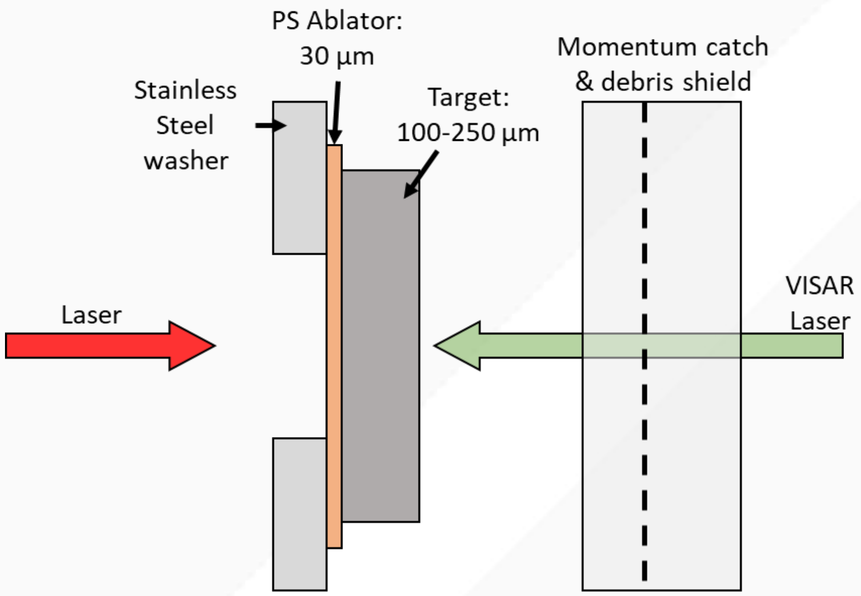

Indirect

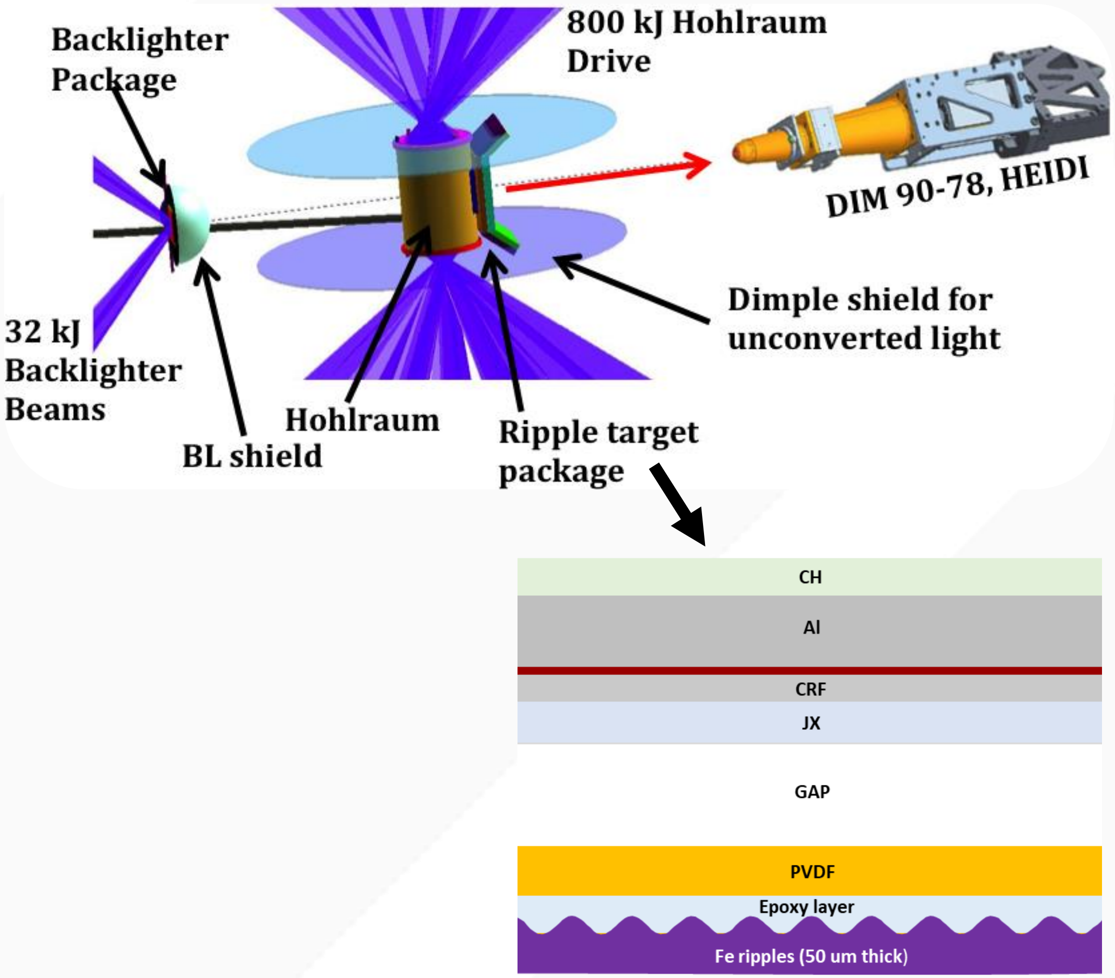

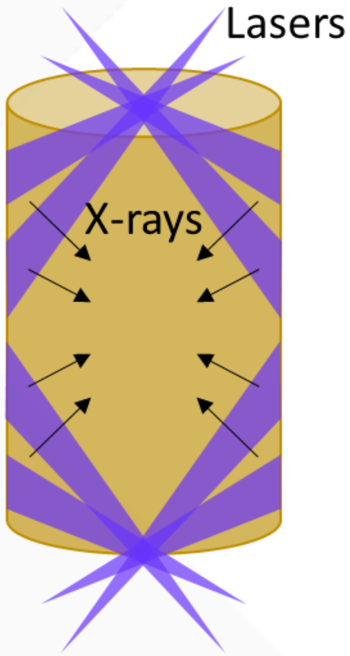

Ramp compression can achieve higher pressures with lower temperature.

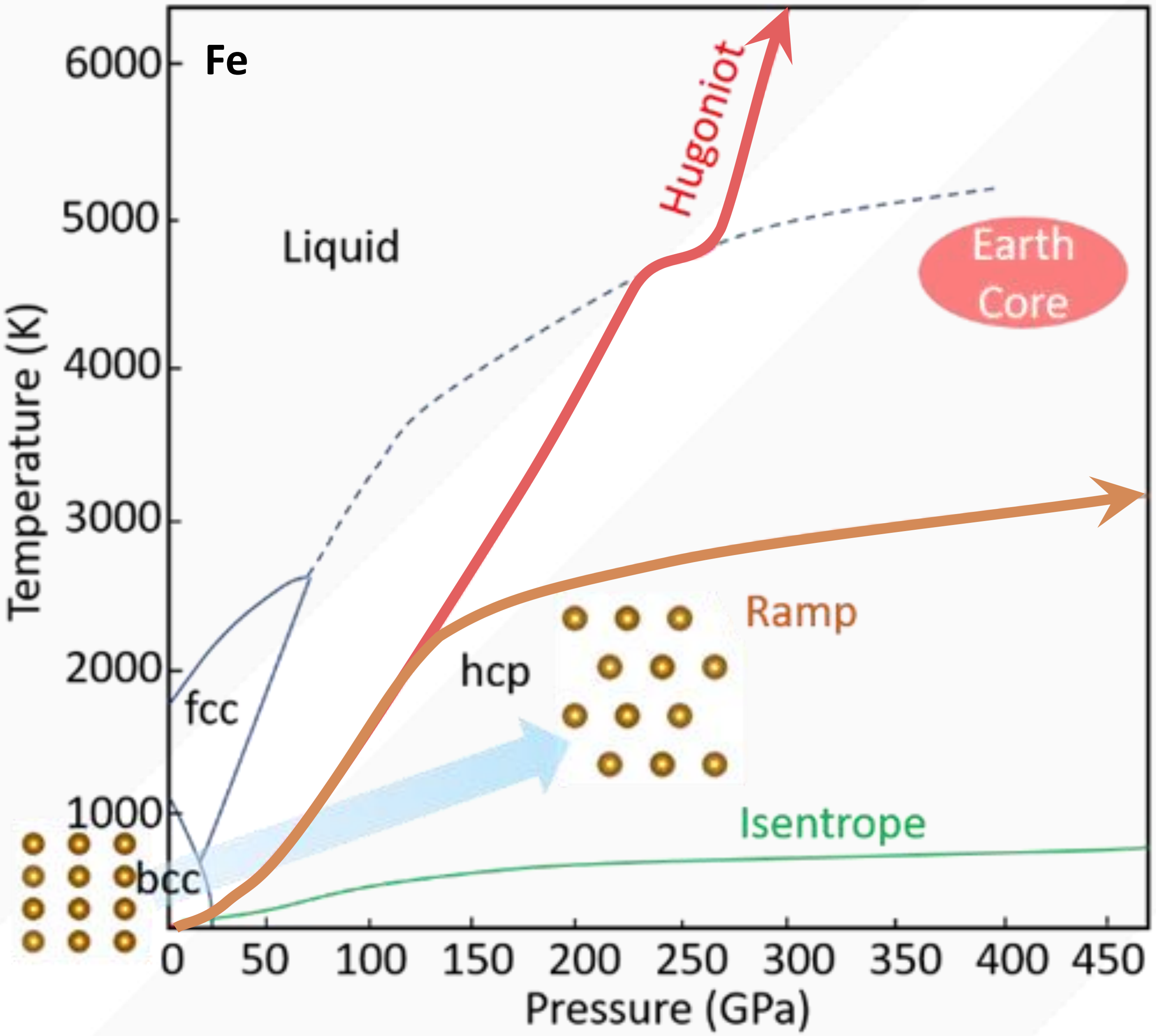

Shock compression:
T_{350GPa} = >6000 K → melted!

Ramp compression:
T_{350GPa} = ~3000 K → solid!

Laser facilities across the world are used to achieve extreme conditions.

Jupiter Laser Facility
LLNL

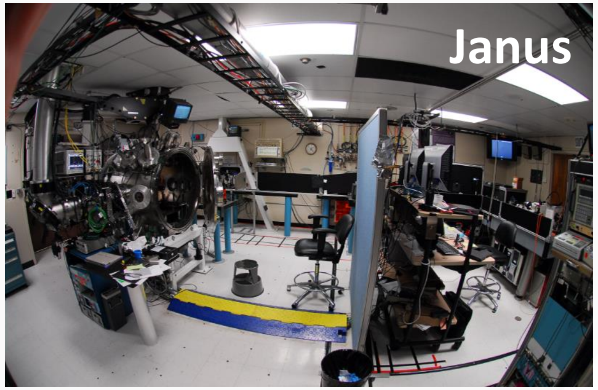

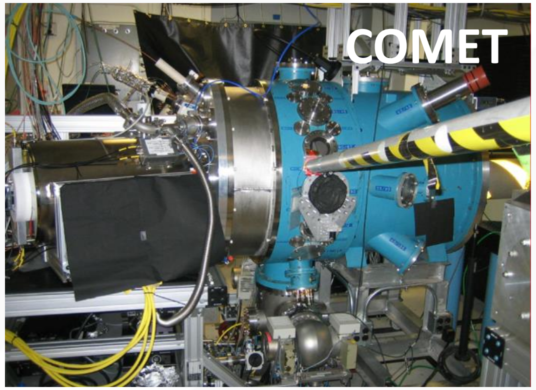

Omega Laser Facility
LLE, University of Rochester

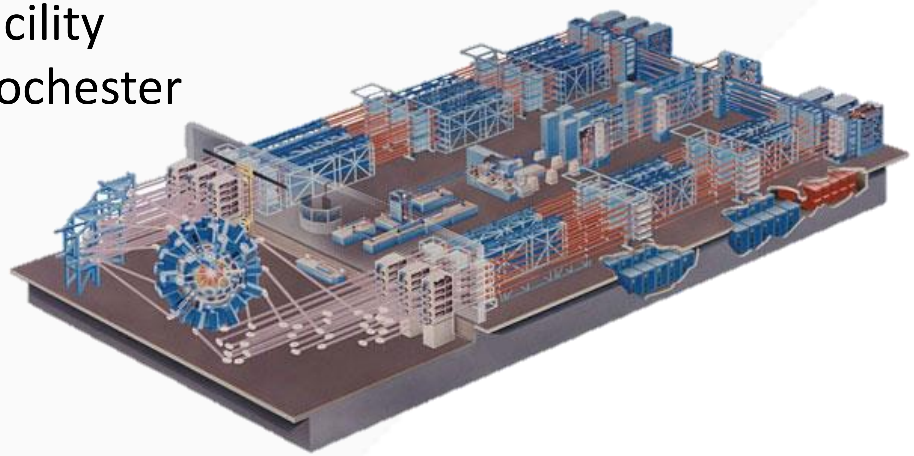

National Ignition Facility
LLNL

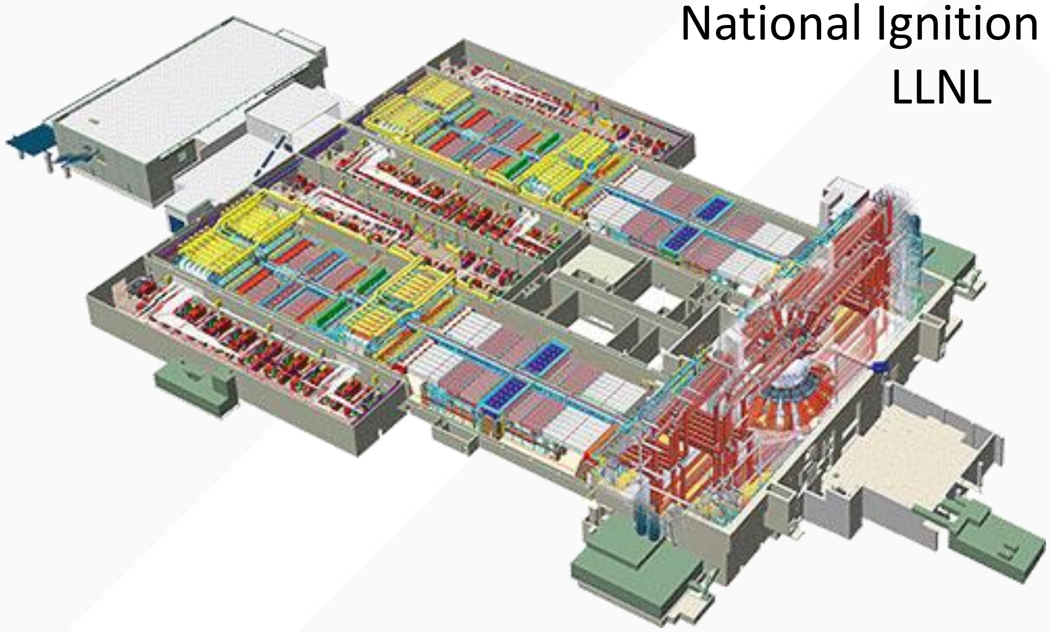

https://lasers.llnl.gov/about/what-is-nif
http://www.lle.rochester.edu/omega_facility/omega/
https://jlf.llnl.gov/laser-facilities

Rankine-Hugoniot equations describe shock behavior of materials.

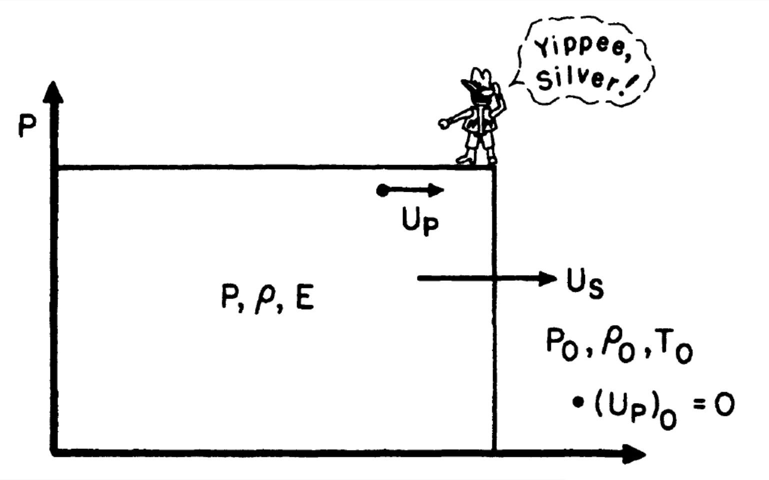

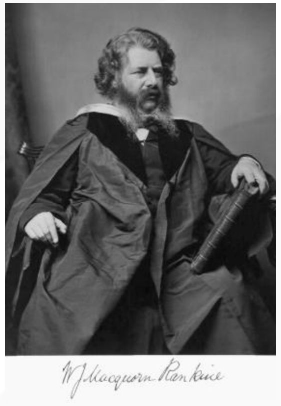

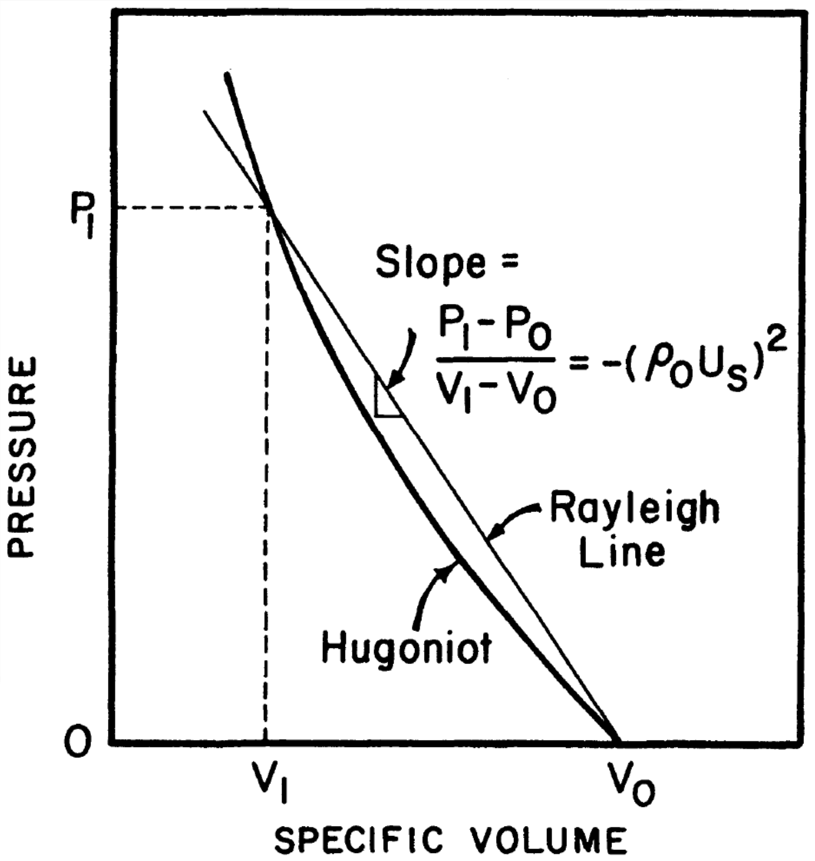

Conservation of mass $\rho_0 U_s = \rho(U_s - U_p)$

Conservation of momentum $P - P_0 = \rho_0 U_s U_p$

Conservation of energy $E - E_0 = \frac{1}{2}(P + P_0)(V_0 - V)$

Equation of State $U_s = C_0 + S_1 U_p + S_2 U_p^2 + \ldots$

Meyers, M.A., 1994. Dynamic Behavior of Materials, J. Wiley.
Rankine, W. J. M., 1870, *Philosophical Transactions of the Royal Society of London.*
Hugoniot. H. J., 1889, *Journal de L'Ecole Polytechnique.*

Slip and twinning are competing deformation mechanisms

Hall Petch Equation:

$$\boldsymbol{\sigma_{T\ or\ S} = \sigma_o + k_{T\ or\ S} d^{-1/2}}$$

$$k_{twinning} > k_{slip}$$

Twinning:

$$\boldsymbol{\sigma_T = K\dot{\epsilon}^{1/m+1}\, exp\left[\frac{Q}{(m+1)RT}\right]}$$

$$\boldsymbol{K = M_T\left(\frac{nlE}{MA_0}\right)^{1/m+1}}$$

Slip (Zerilli-Armstrong constitutive eqn):

$$\boldsymbol{\sigma_S = \sigma_G + C_1\, exp\left[-\left(C_3 - C_4 ln\frac{\dot{\epsilon}}{\dot{\epsilon}_0}\right)T\right]}$$

If $\boldsymbol{\sigma_S = \sigma_T}$:

$$\boldsymbol{-\sigma_G + K\dot{\epsilon}^{1/m+1}\, \mathbf{exp}\left[\frac{Q}{(m+1)RT}\right] - C_1\, \mathbf{exp}\left[-\left(C_3 - C_4 ln\frac{\dot{\epsilon}}{\dot{\epsilon}_0}\right)T\right] + \sigma_{T0} - \sigma_{S0} + (k_T - k_S)d^{-1/2} = 0}$$

M. A. Meyers, O. Vöhringer, and V. A. Lubarda, *Acta Materialia*, vol. 49, no. 19, (2001).
Armstrong, R. W. and Worthington, P. J., in Metallurgical Effects at High Strain Rates, ed. R. W. Rohde, B. M. Butcher, J. R. Holland and C. H. Karnes. Plenum Press, New York, 1973, pp. 401–414.

Slip and twinning are competing deformation mechanisms

If $\sigma_S = \sigma_T$:

$$-\sigma_G + K\dot{\epsilon}^{1/m+1} \exp\left[\frac{Q}{(m+1)RT}\right] - C_1 \exp\left[-\left(C_3 - C_4 ln\frac{\dot{\epsilon}}{\dot{\epsilon}_0}\right)T\right] + \sigma_{T0} - \sigma_{S0} + (k_T - k_S)d^{-1/2} = 0$$

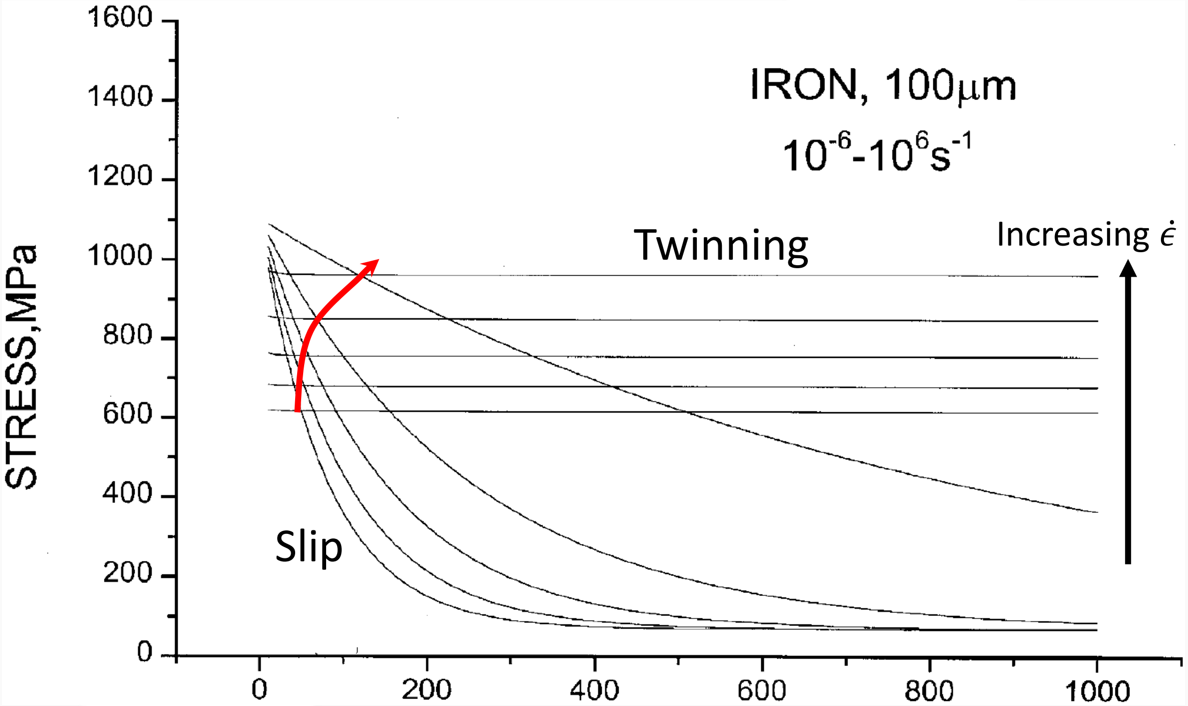

- Transition stress increases with strain rate

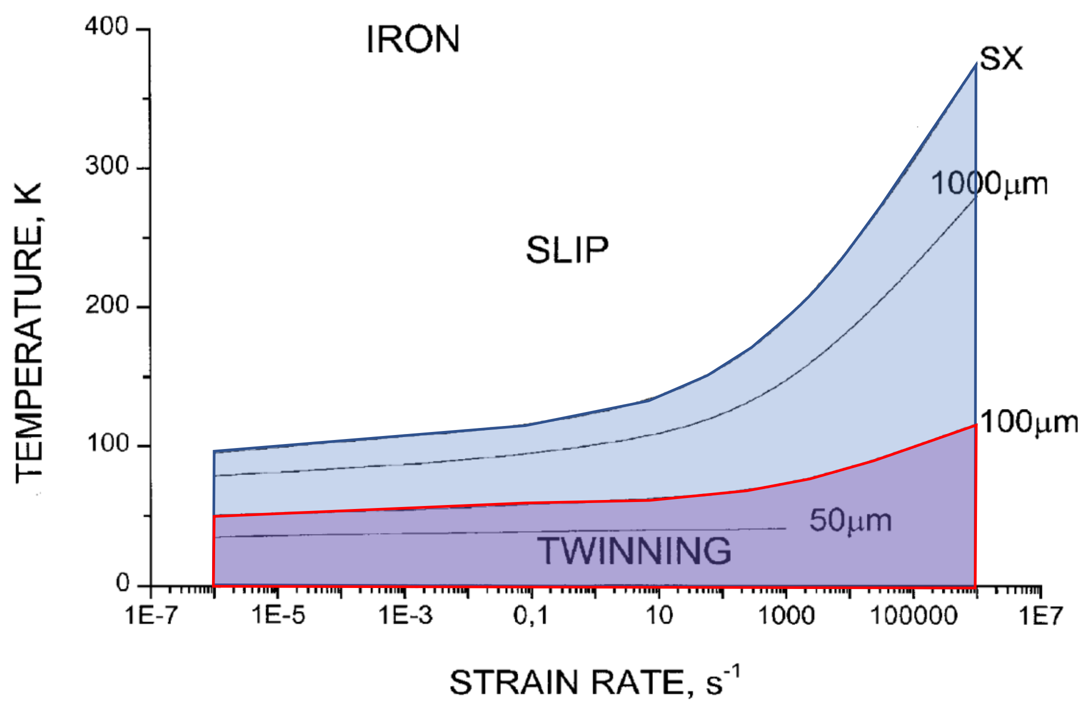

- Twinning domain increases with larger grains size

M. A. Meyers, O. Vöhringer, and V. A. Lubarda, *Acta Materialia*, vol. 49, no. 19, (2001)
M.A., Meyers, R.W., Armstrong, H.O.K., Kirchner, Mechanics and Materials: fundamentals and linkages, *J. Wiley* (1999).

Material strength can be modeled using flow relationships:

Voce strain hardening

$$\frac{d\hat{\tau}}{d\epsilon} = \theta \frac{\hat{\tau}_s - \hat{\tau}}{\hat{\tau}_s - \hat{\tau}_y}$$

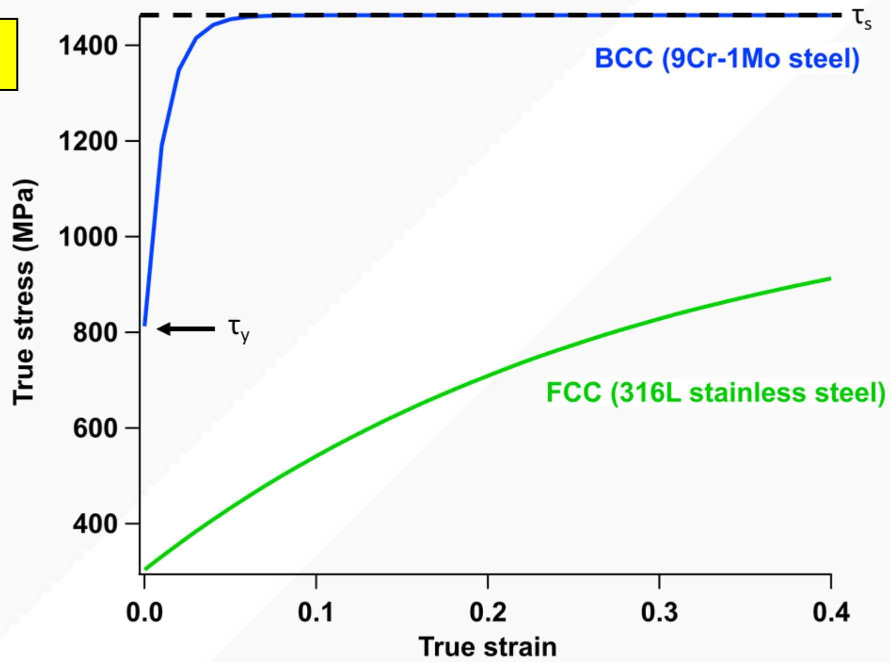

Steinberg-Guinan model

P,T dependent constitutive model

$$\hat{\tau}_y = \hat{\tau} f(\epsilon)\left[1 + \frac{AP}{\eta^{\frac{1}{3}}} + B(T - 300)\right]$$

$\eta = V/V_0 = f(P)$

$$P = \frac{C_0^2 (V_0 - V)}{\left[V_0^2 - S(V_0 - V)\right]^2}$$

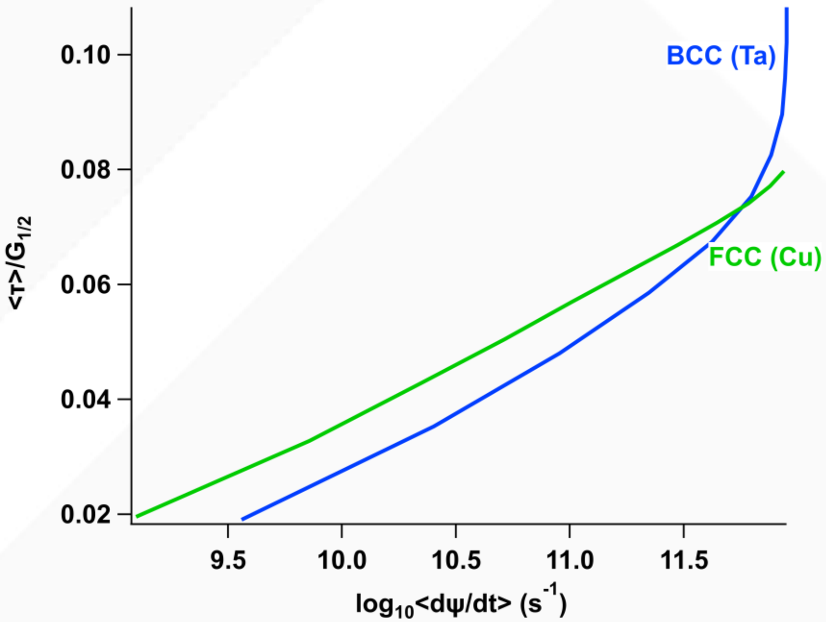

Preston-Tonks-Wallace model

Strain rate dependence added

$$\hat{\tau} = \hat{\tau}_s + \frac{1}{p}(s_0 - \hat{\tau}_y) ln\left\{1 - \left[1 - exp\left(-p\frac{\hat{\tau}_s - \hat{\tau}_y}{s_0 - \hat{\tau}_y}\right)\right] exp\left[-\frac{p\theta\epsilon}{(s_0 - \hat{\tau}_y)\left[exp\left(p\frac{\hat{\tau}_s - \hat{\tau}_y}{s_0 - \hat{\tau}_y}\right) - 1\right]}\right]\right\}$$

$\hat{\tau}_s, \hat{\tau}_y = f(T, \dot{\epsilon}, G)$ $\qquad$ $\dot{\epsilon}$ - strain rate

D.J. Steinberg, S.G. Cochran, and M.W. Guinan, J. Appl. Phys. 51, 1498 (1980)
Preston, D. L., Tonks, D. L. & Wallace, D. C. J. Appl. Phys. 93 (2003).

Dislocation motion controls differing behavior in BCC and FCC metals.

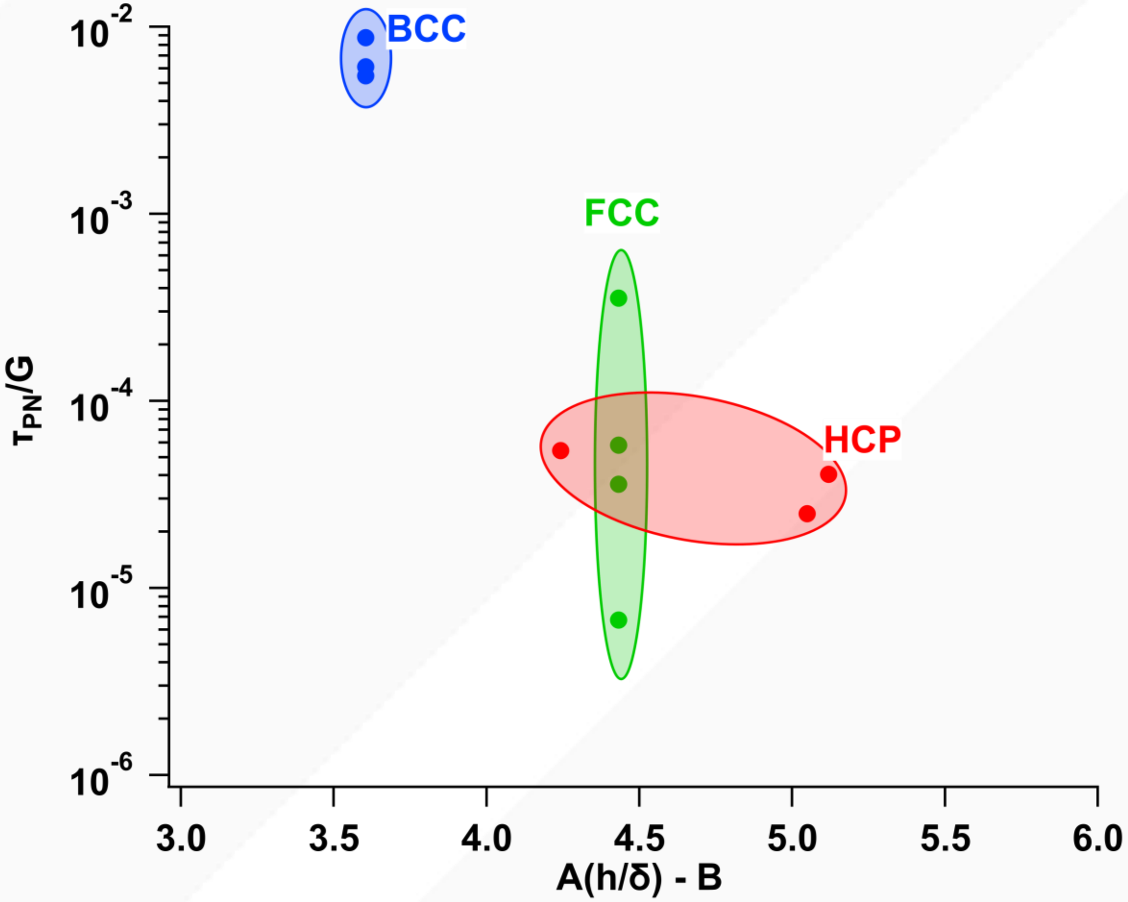

- Stress to initiate dislocations for BCC metals >> FCC or HCP metals

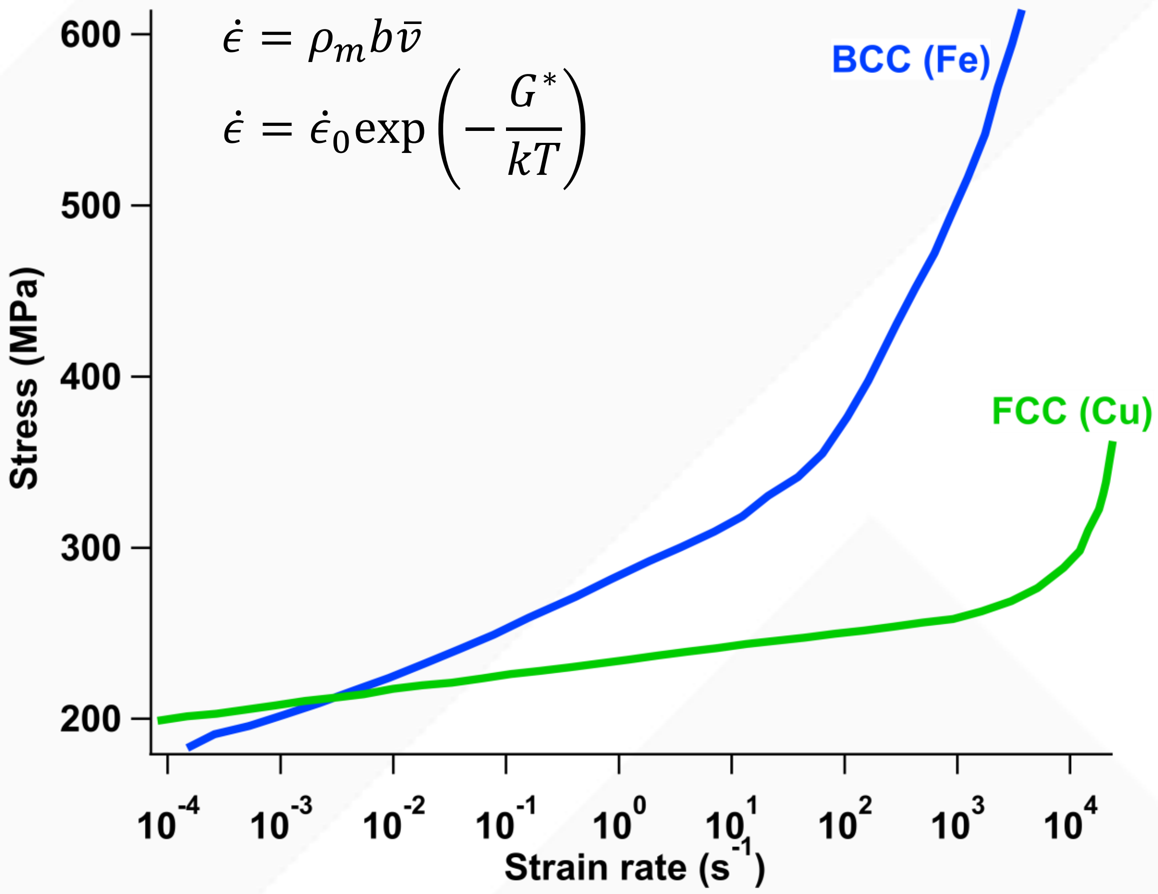

- BCC metals are much more sensitive to strain rate than FCC metals

Meyers, M.A., 1994. Dynamic Behavior of Materials, J. Wiley.
Orowan, E. Problems of plastic gliding. in Proc. Phys. Soc. 1940.

Gas gun experiments investigate post-shock microstructure and extend Hugoniot.

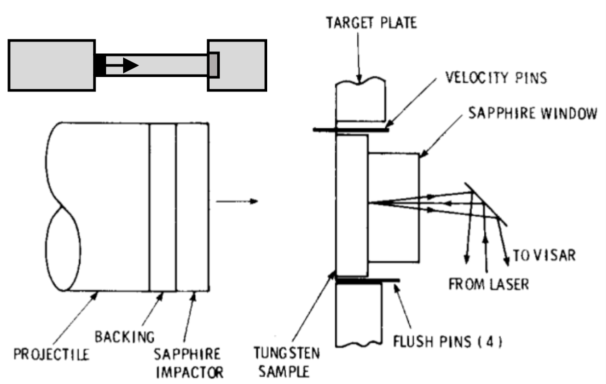

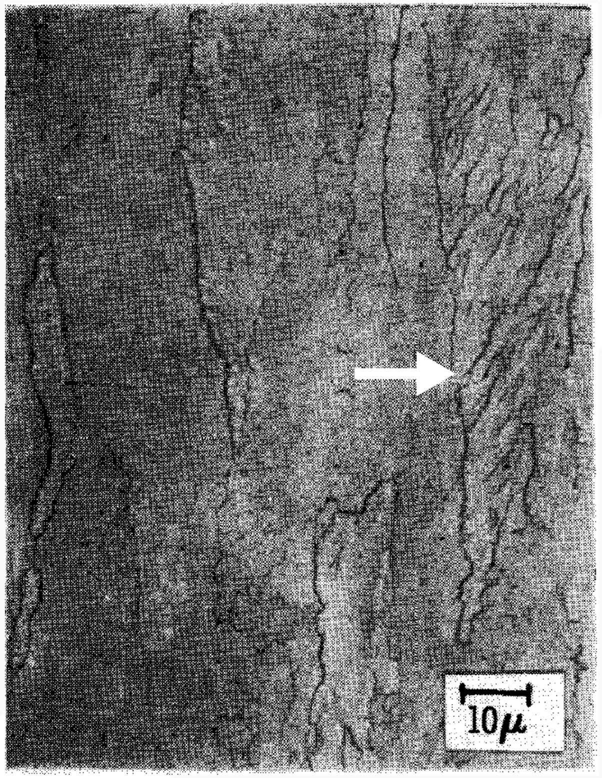

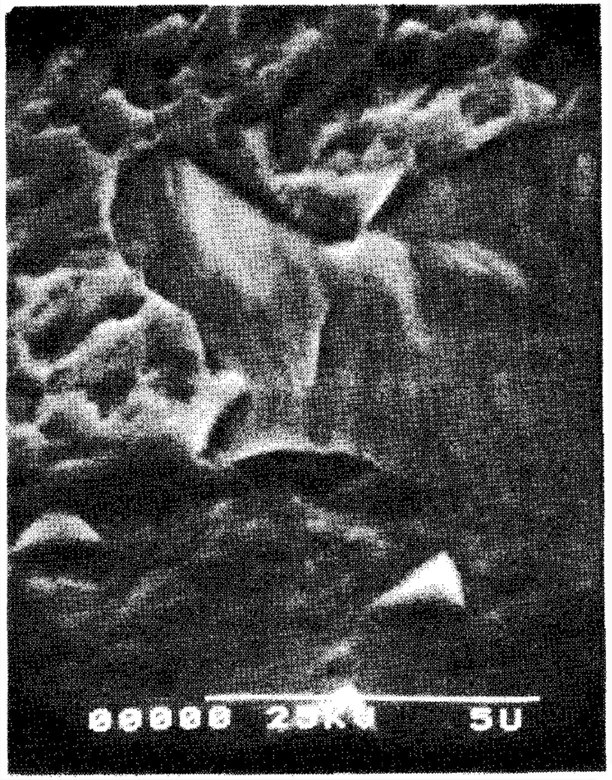

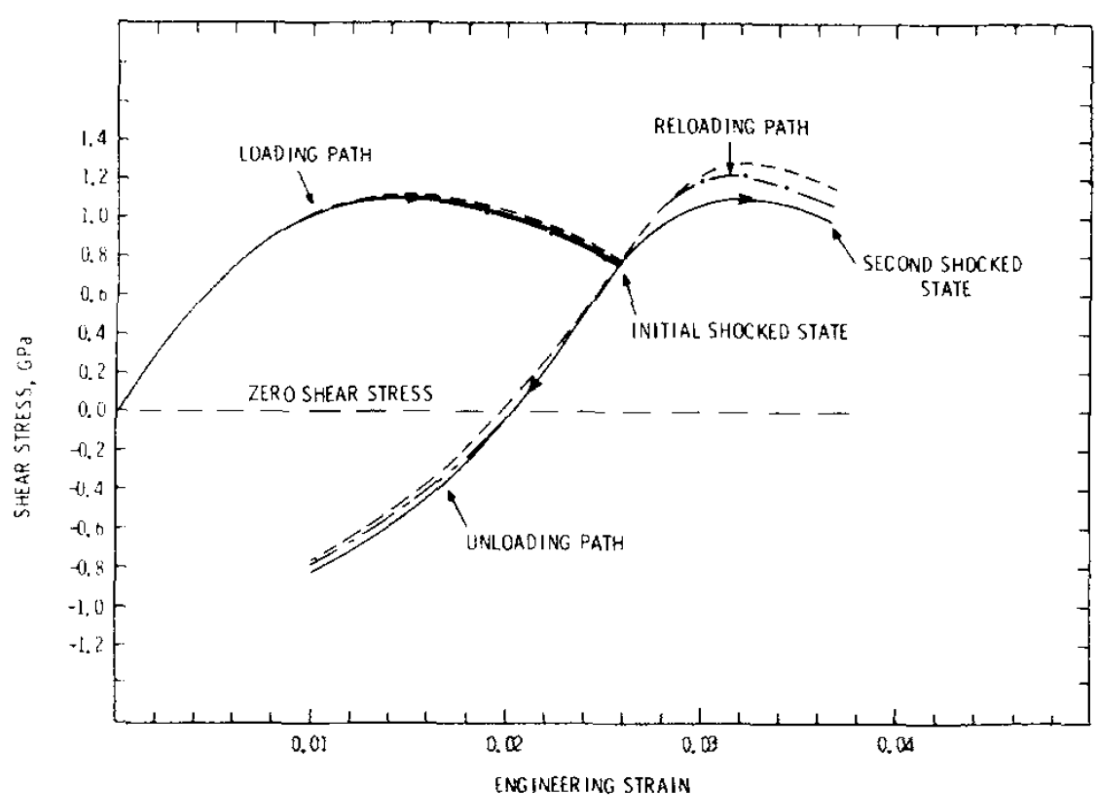

Evidence of both slip and twinning may be responsible for observed softening

J. R. Asay, L. C. Chhabildas, and D. P. Dandekar, *Journal of Applied Physics*, vol. 51, no. 9, (1980).

Stability of BCC phase confirmed through gas gun experiments.

42
Mo

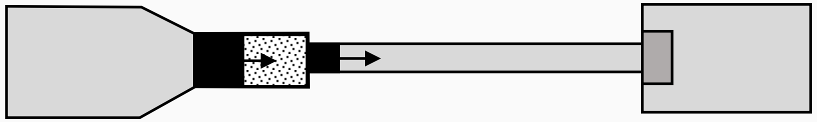

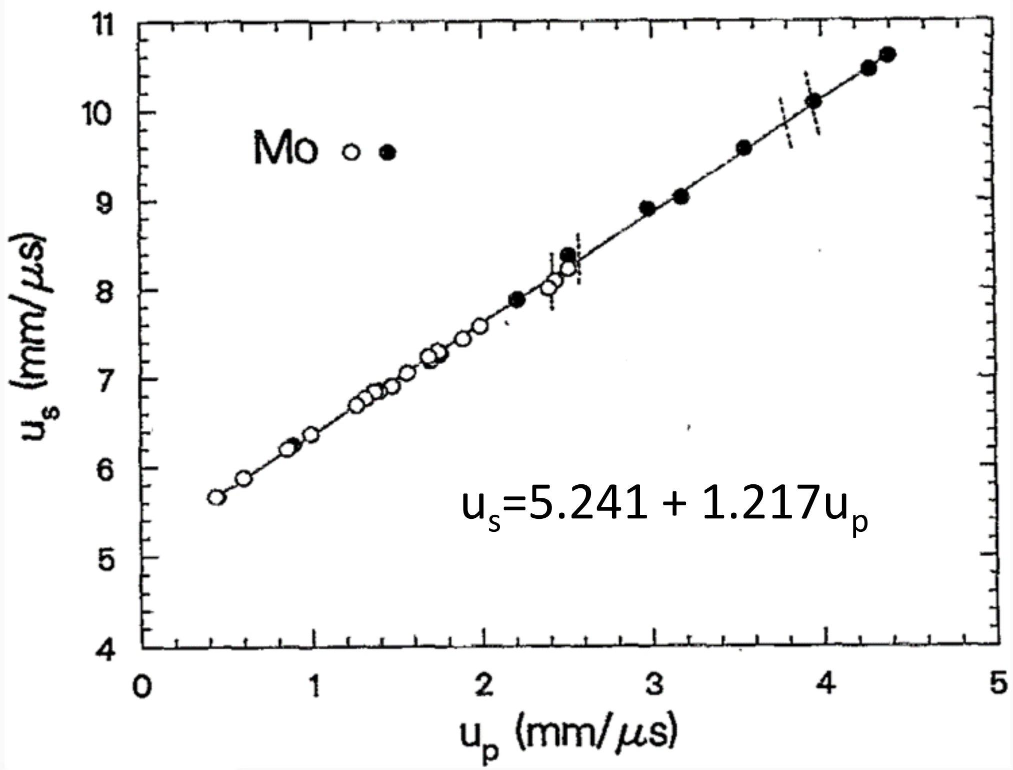

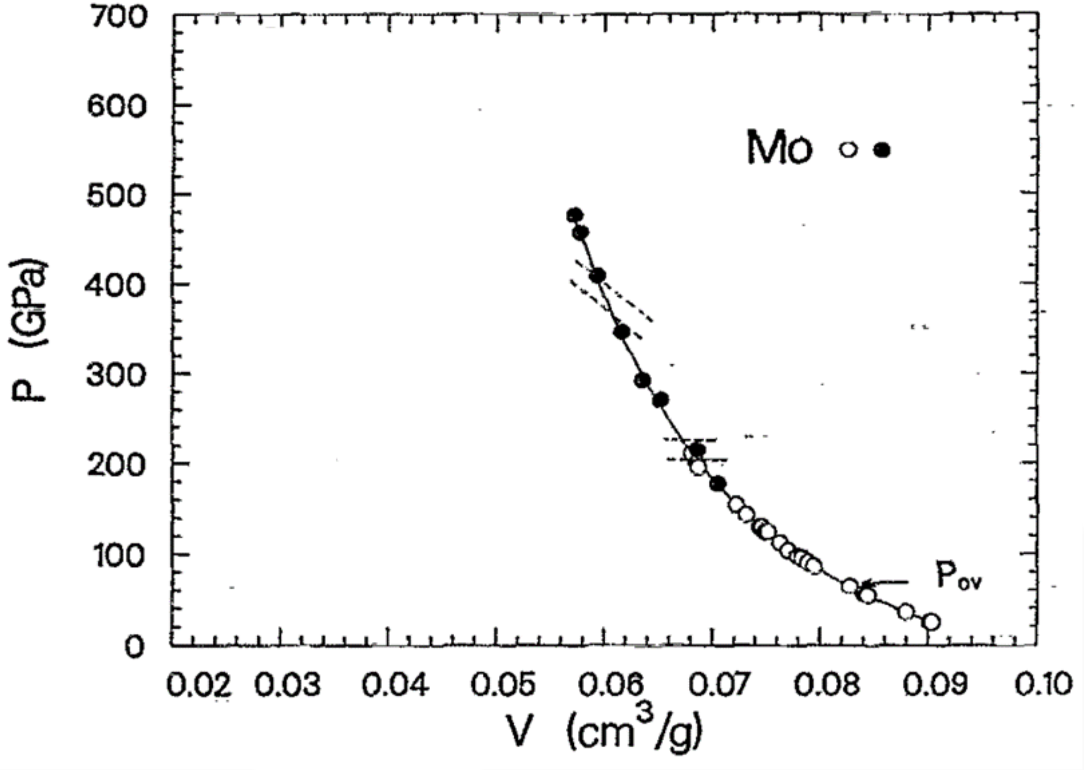

BCC structure stable up to 480 GPa

R. S. Hixson and J. N. Fritz, *Journal of Applied Physics*, vol. 71, no. 4, (1992).

Ramp and shock compression also confirm stability of BCC phase.

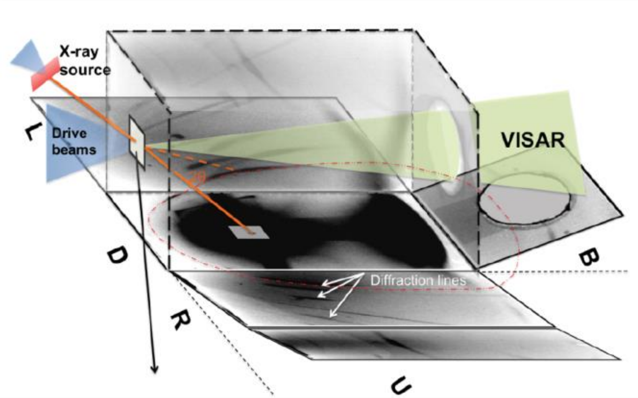

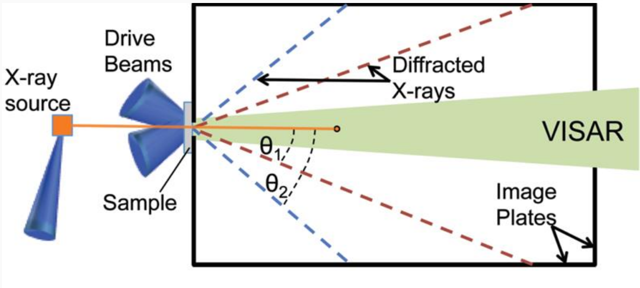

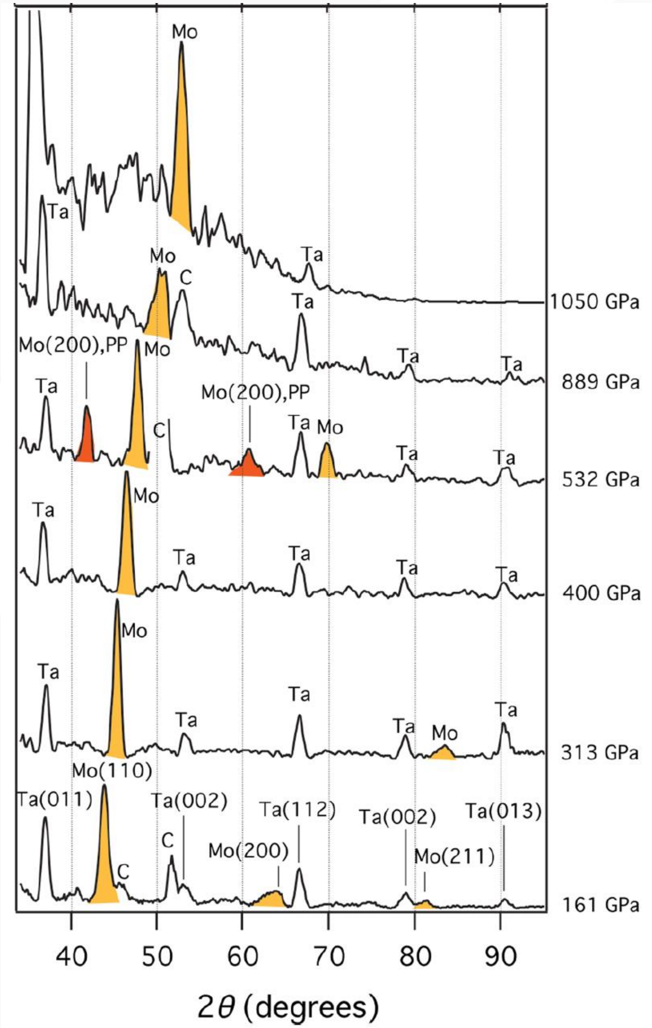

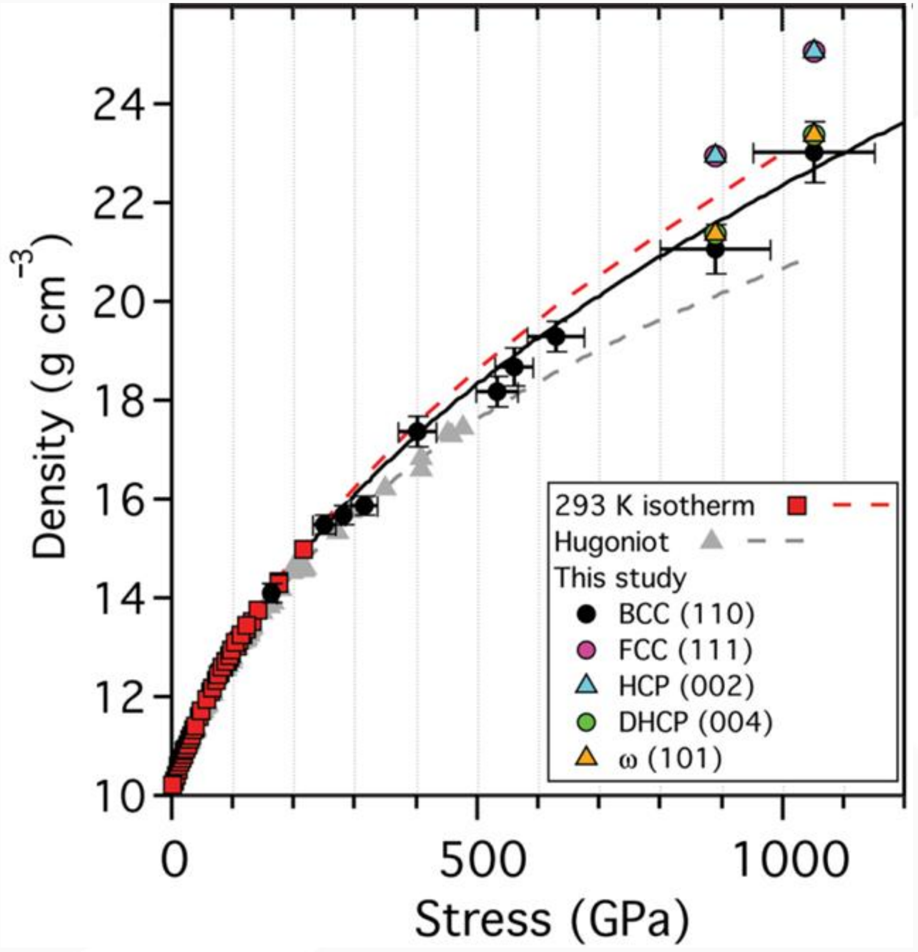

BCC structure stable to 1050 GPa under ramp compression or until shock melting at 390 GPa.

J. Wang *et al.*, *Phys. Rev. B*, vol. 92, no. 17, (2015).
J. Wang *et al.*, *Phys. Rev. B*, vol. 94, no. 10, (2016).

Phonon drag mechanism proposed to explain high effective lattice viscosity.

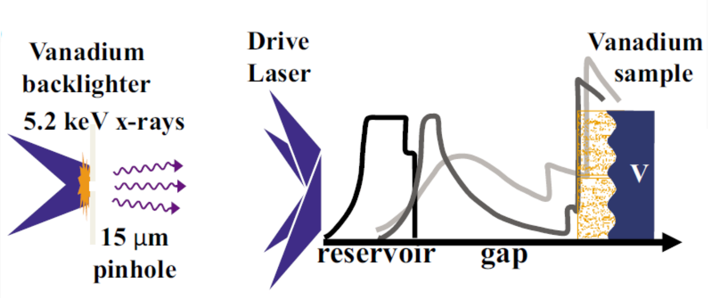

Strong RT instability stabilization points to phonon drag mechanism

(resistance to the dislocation motion can come from scattering of lattice phonons)

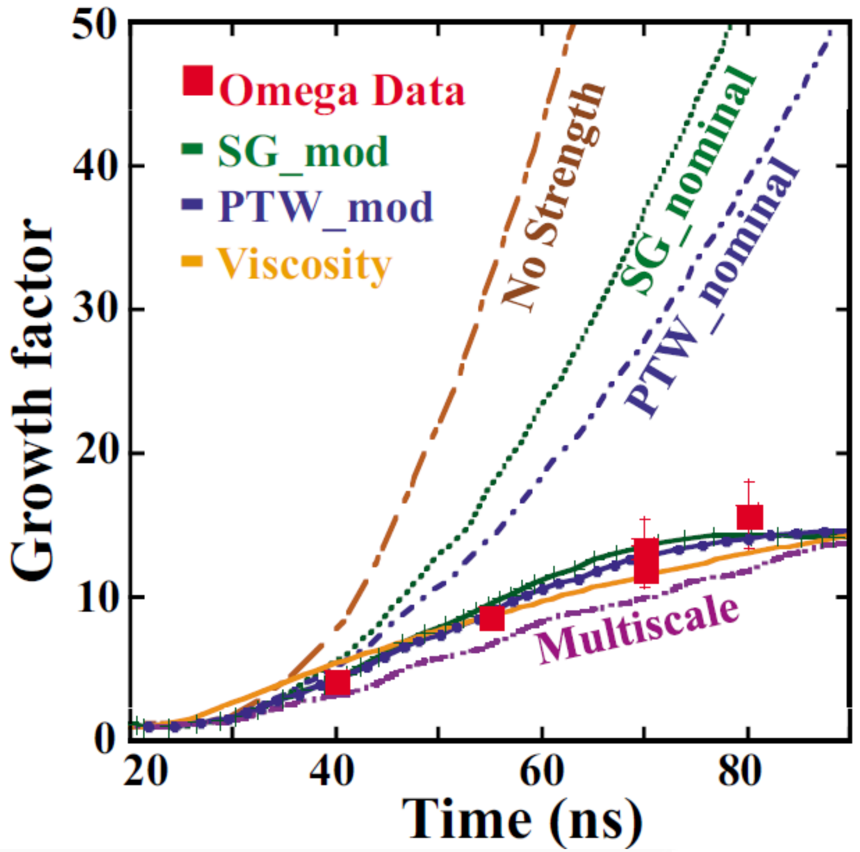

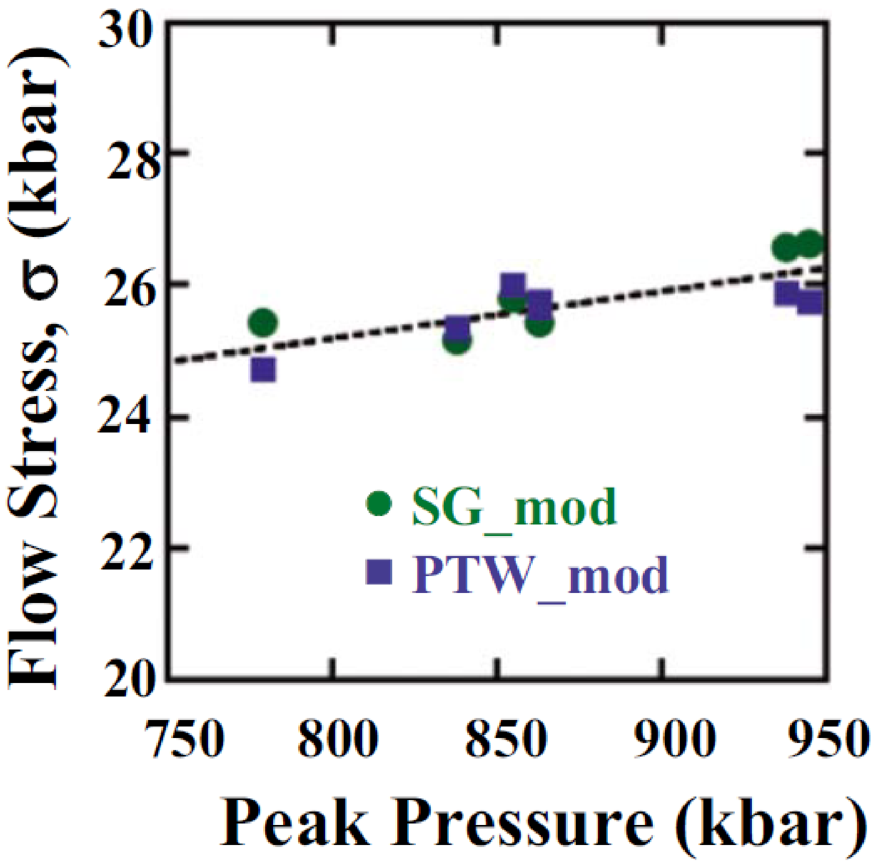

H.-S. Park *et al.*, *Phys. Rev. Lett.*, vol. 104, no. 13, (2010).
H.-S. Park *et al.*, *Physics of Plasmas*, vol. 17, no. 5, (2010).

Contradictions to Hall-Petch relationship suggest different fracture theory.

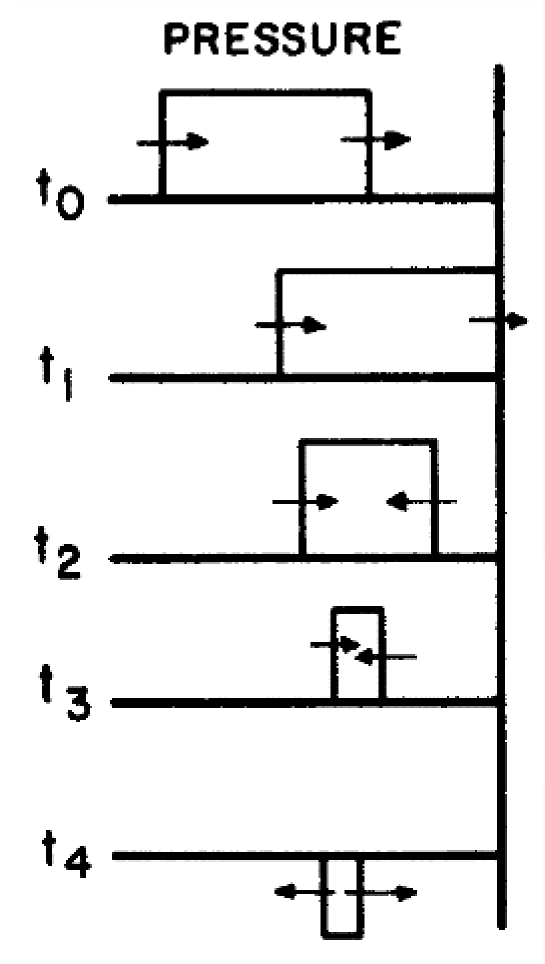

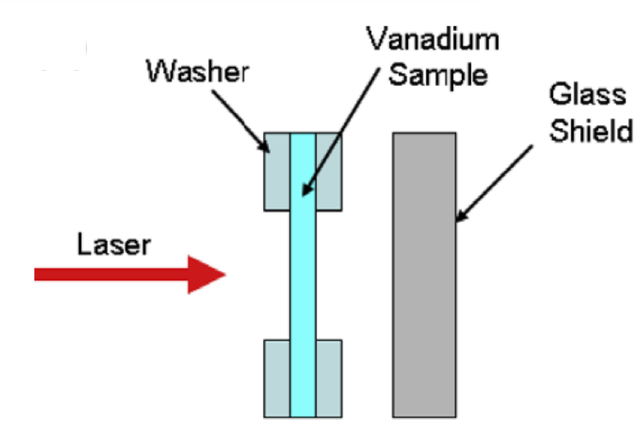

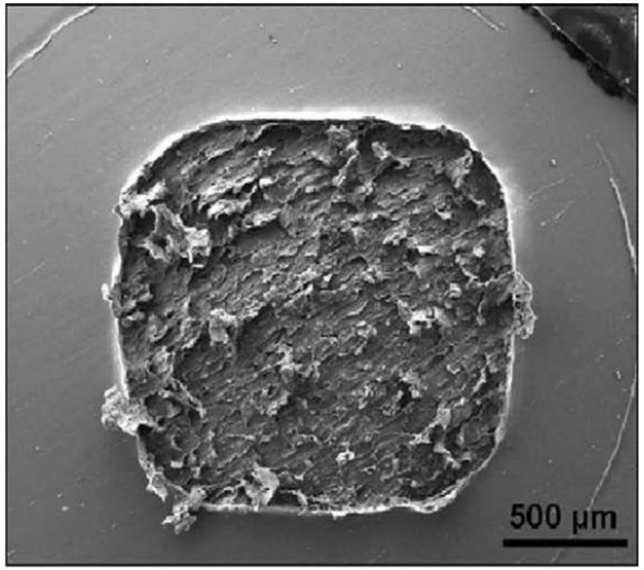

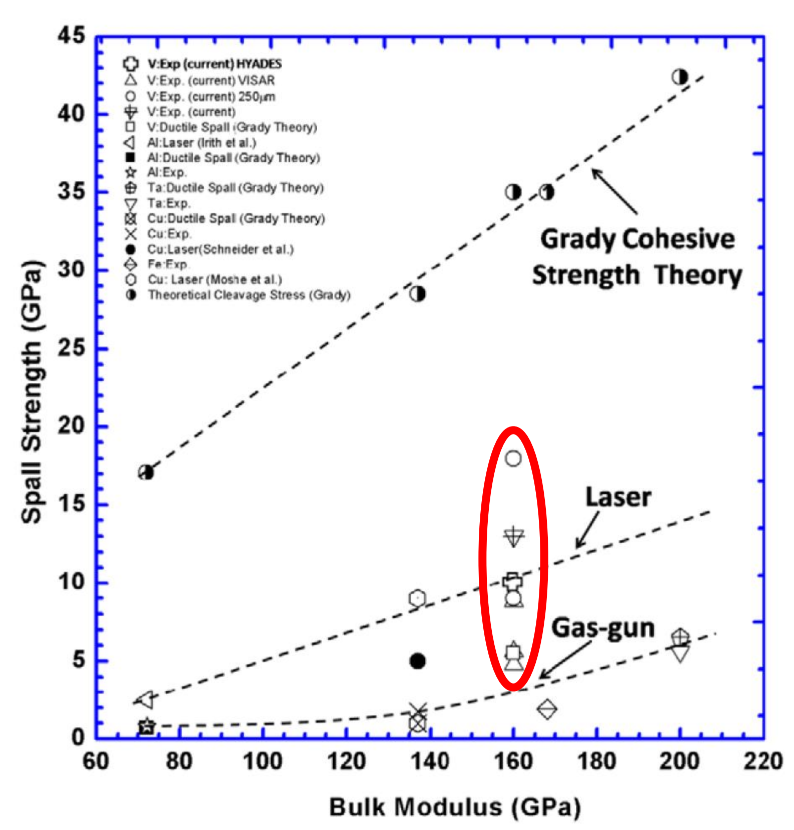

$$\sigma_{sp}^{poly} < \sigma_{sp}^{mono}$$

Strong time dependence
-> Grady Theory

H. Jarmakani, et al., *Acta Materialia*, vol. 58, no. 14, (2010).

Slip-twinning threshold stress dependence on grain size in tantalum.

73
Ta

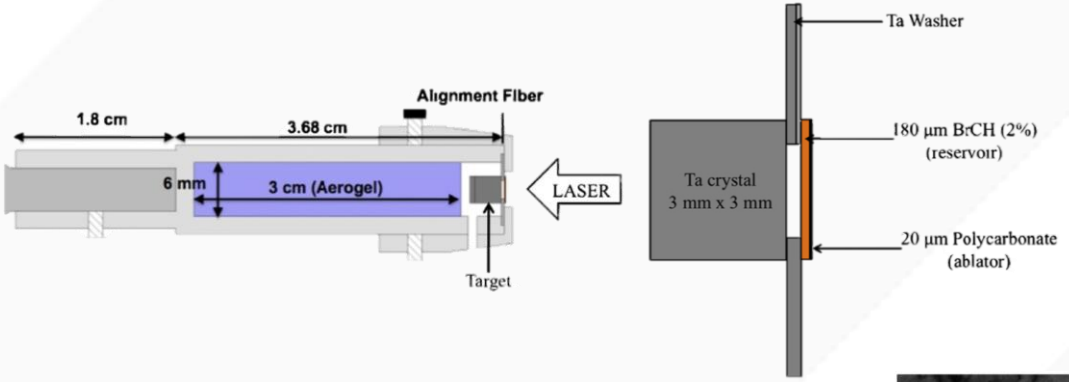

$\sigma_{th}^{slip-twin}$ increases from ~24 GPa (for mono) to 150 GPa (for nano)

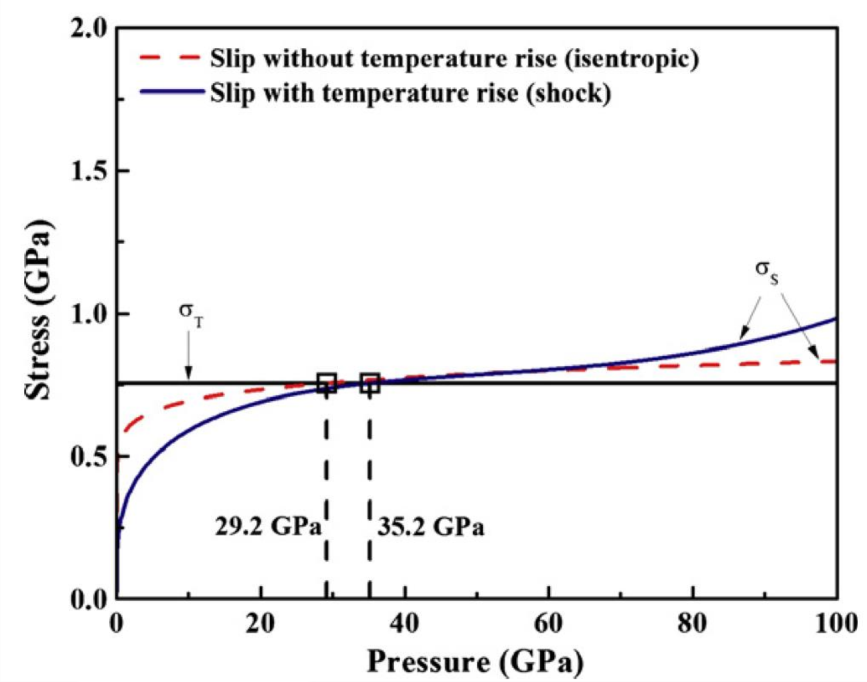

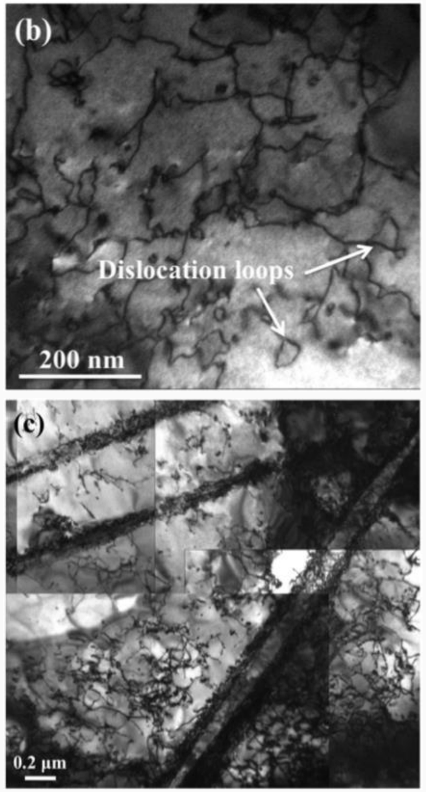

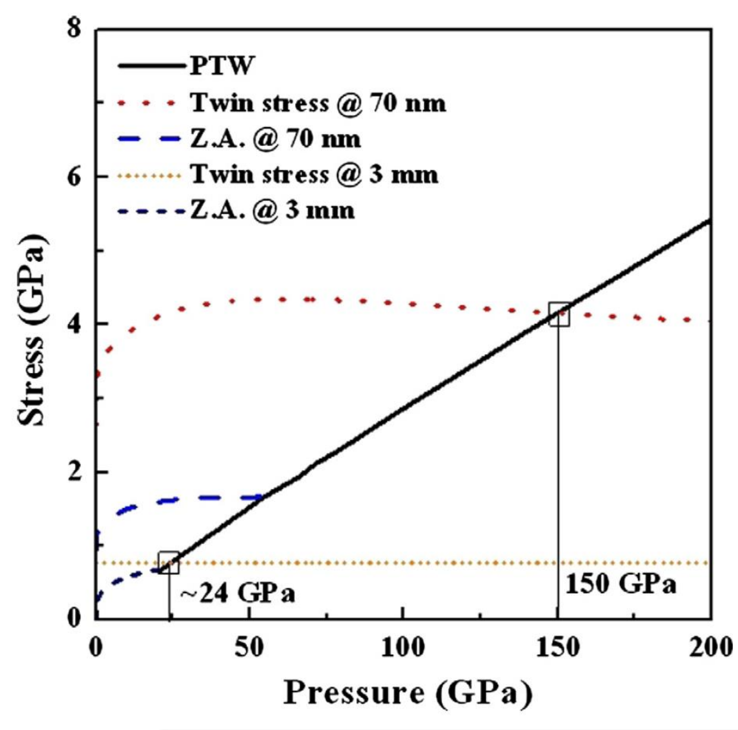

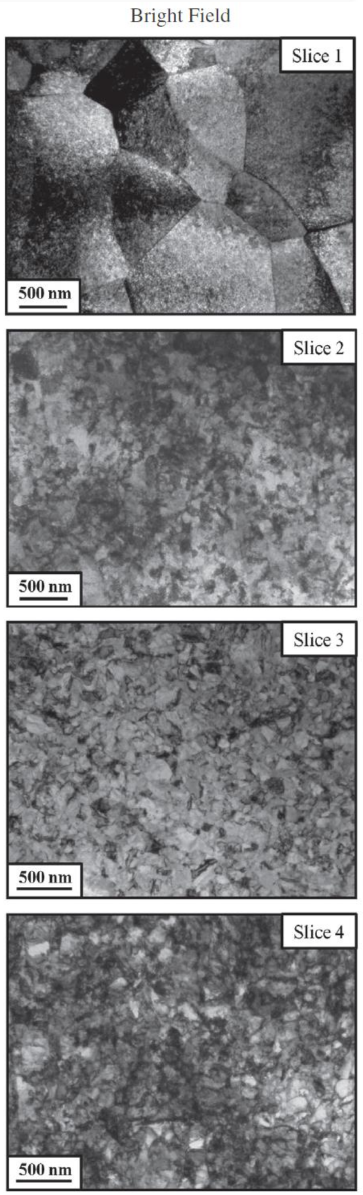

C. H. Lu *et al.*, *Acta Materialia*, vol. 60, no. 19, (2012).

C. H. Lu *et al.*, *Acta Materialia*, vol. 61, no. 20, (2013).

Spall strength is studied using laser shock compression and MD simulations.

73
Ta

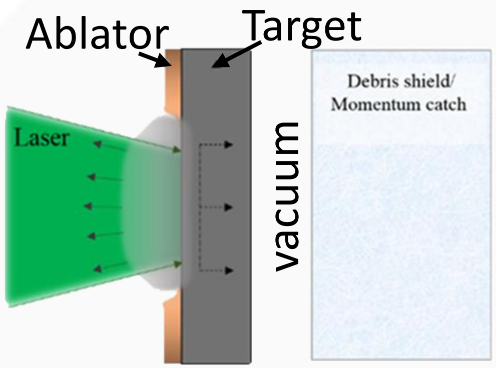

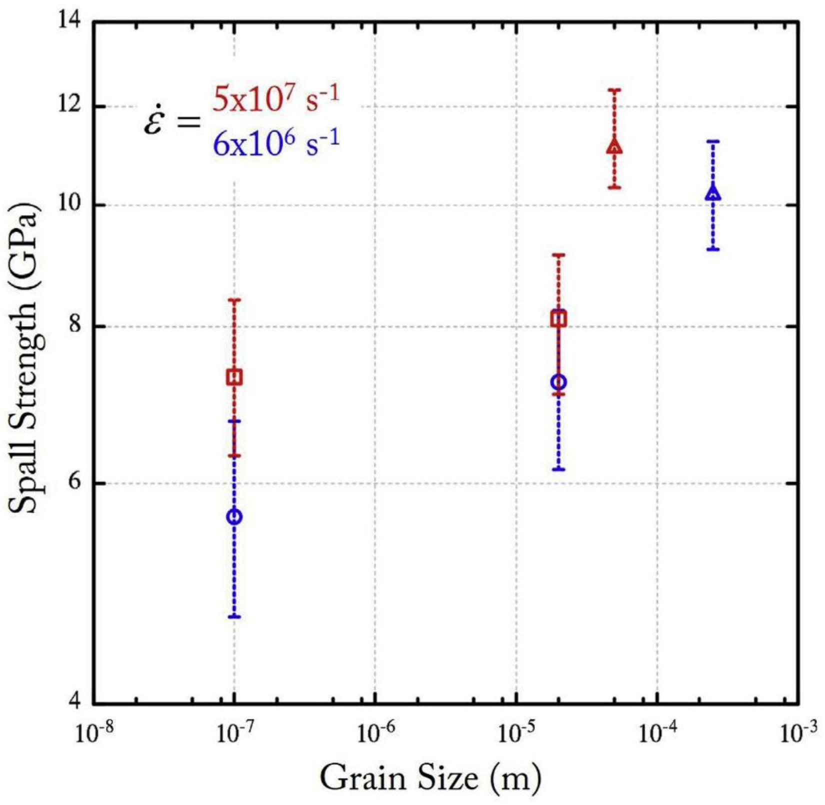

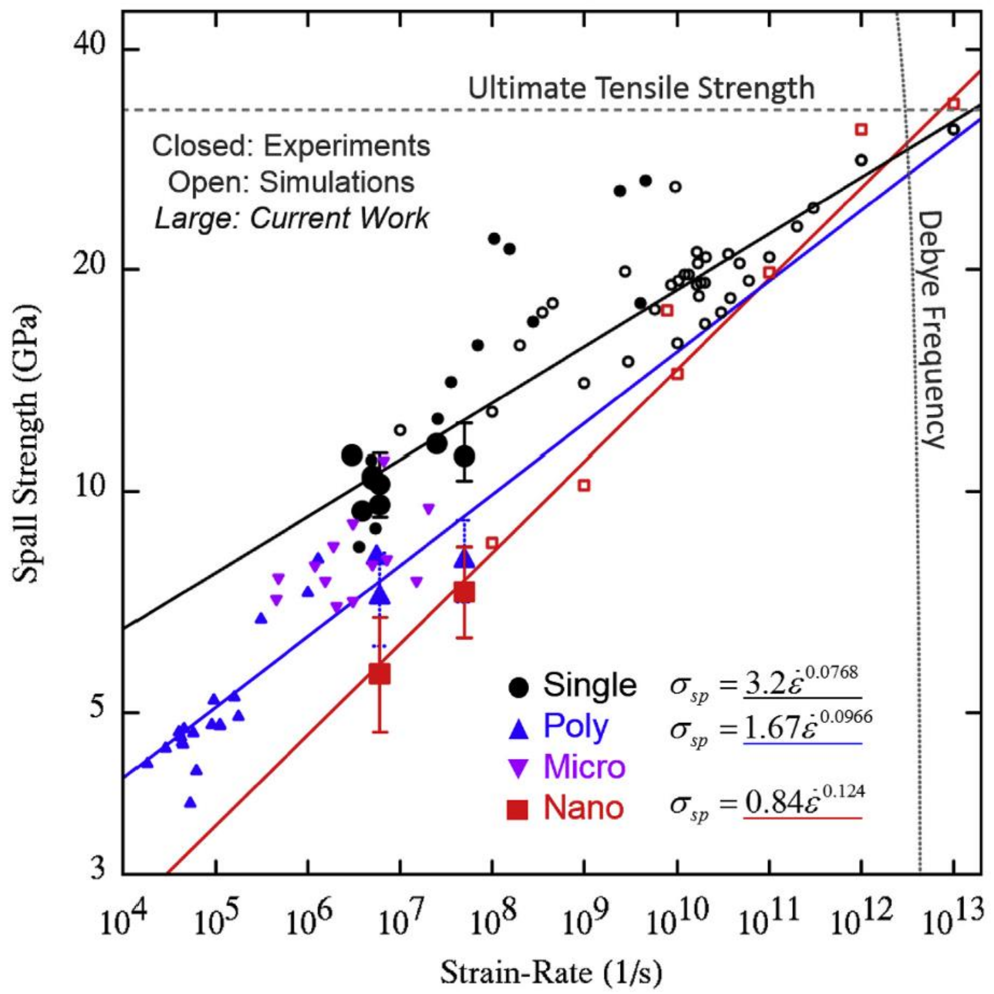

Curran-Seaman-Shockey theory explains $\sigma_{sp}^{mono} > \sigma_{sp}^{nano}$

T. P. Remington *et al.*, *Acta Materialia*, vol. 158, (2018).

Spall strength is studied using laser shock compression and MD simulations.

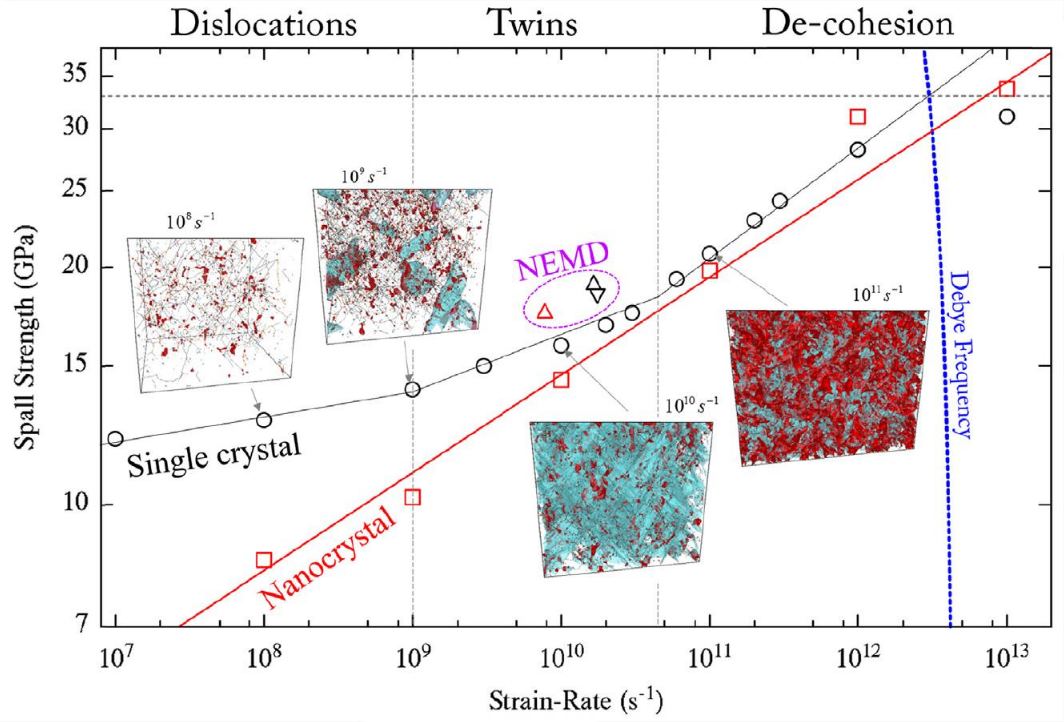

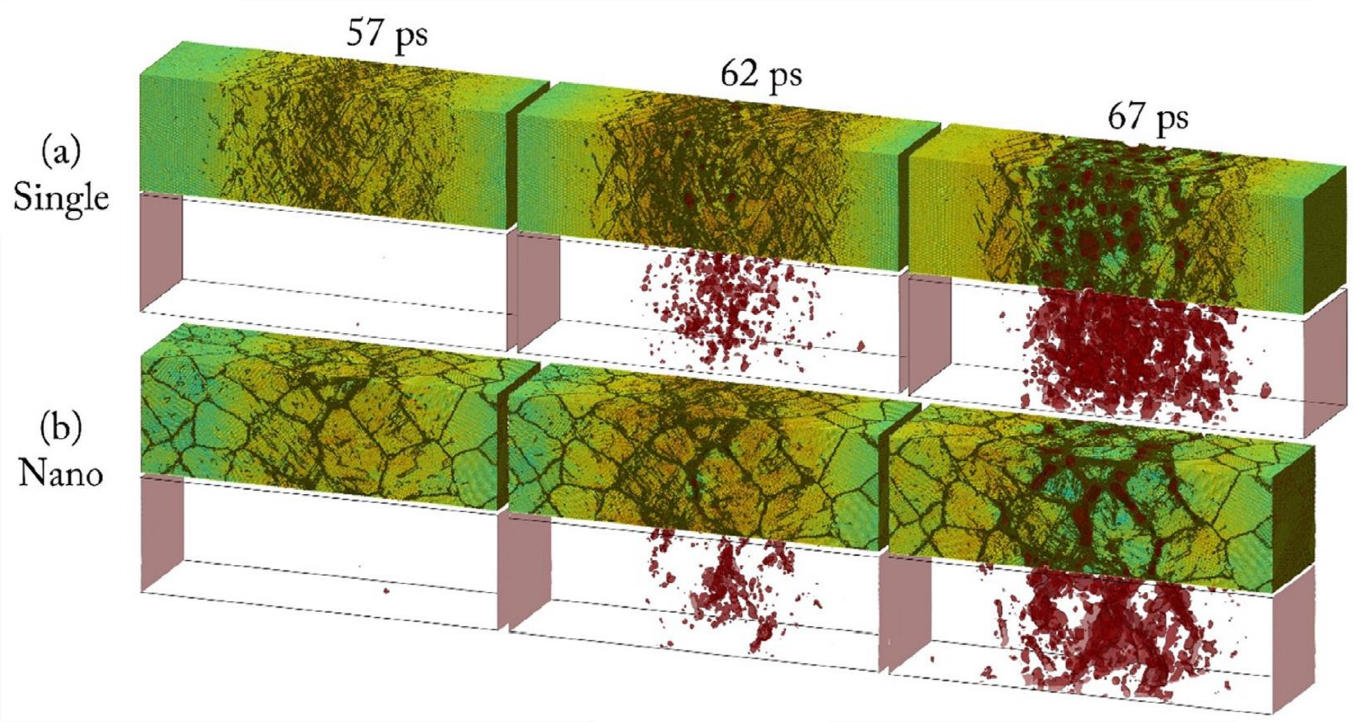

Single crystals

low strain rates: dislocations are dominant mechanism, with increasing strain rate more dislocations form and end up producing twins

high strain rates: failure by de-cohesion of atoms

Nanocrystal

Single dominant deformation mechanism: grain-boundary nucleation of voids, limited dislocation and twin nucleation

E. N. Hahn, et al., *Acta Materialia*, vol. 126, (2017).

Rayleigh-Taylor and Richtmyer-Meshkov instabilities used to measure strength.

73
Ta

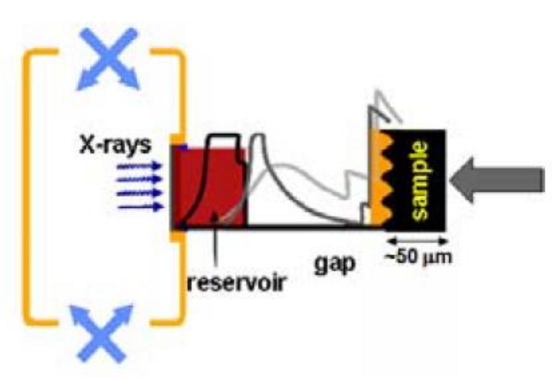

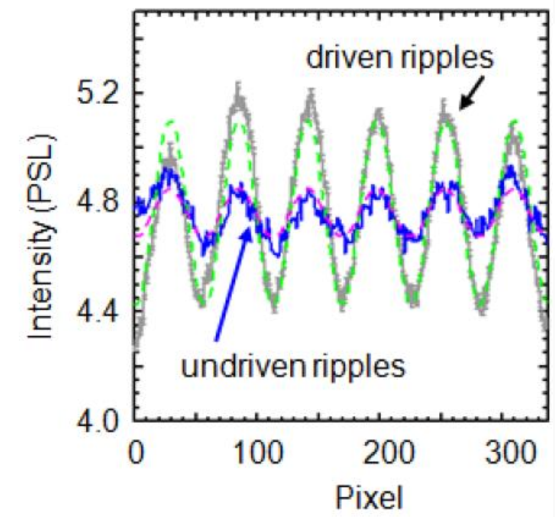

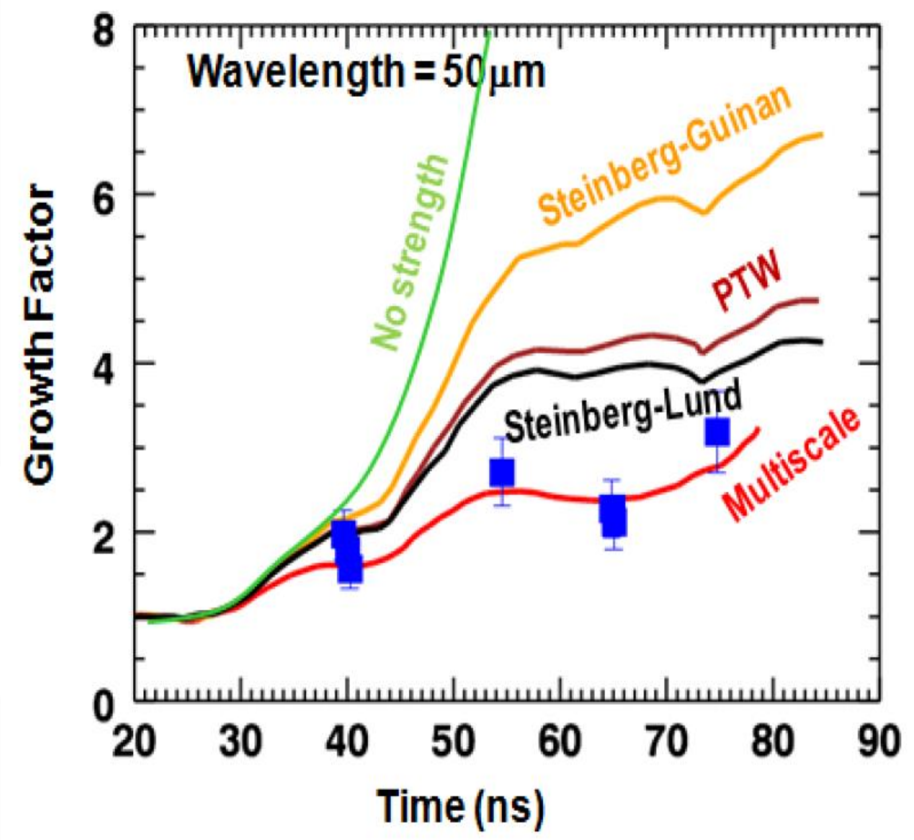

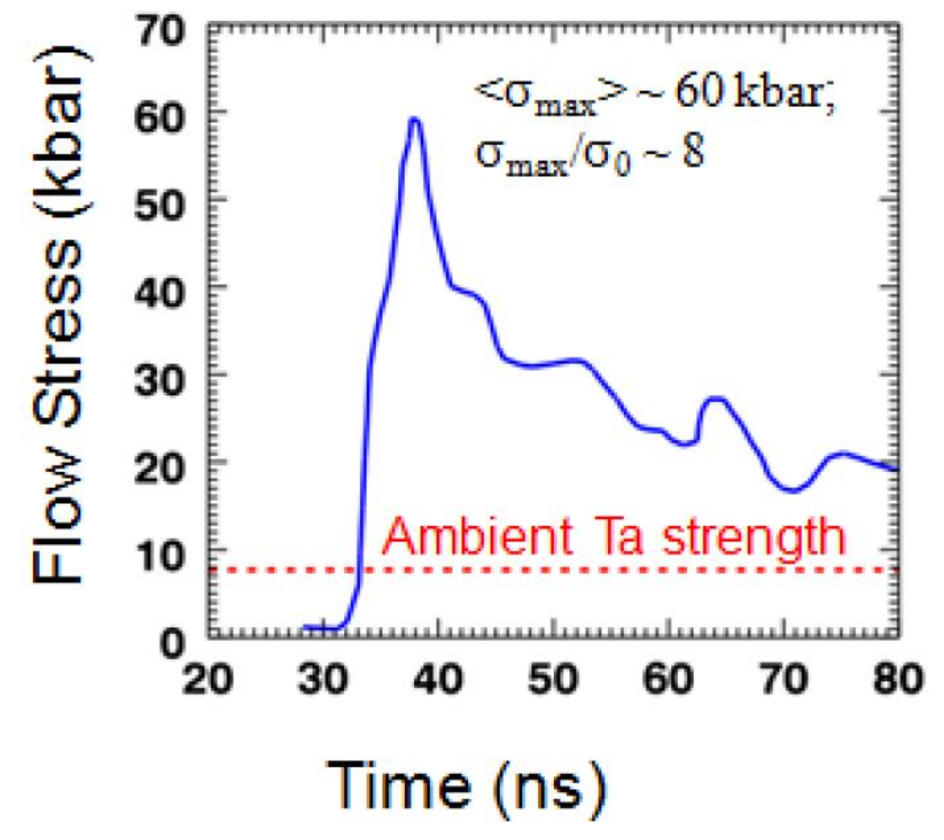

High pressure strength ~8x ambient value

H.-S. Park *et al.*, presented at the SHOCK COMPRESSION OF CONDENSED MATTER (2012).

Rayleigh-Taylor and Richtmyer-Meshkov instabilities used to measure strength.

73
Ta

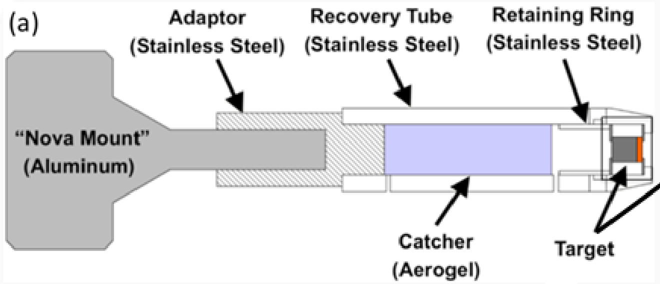

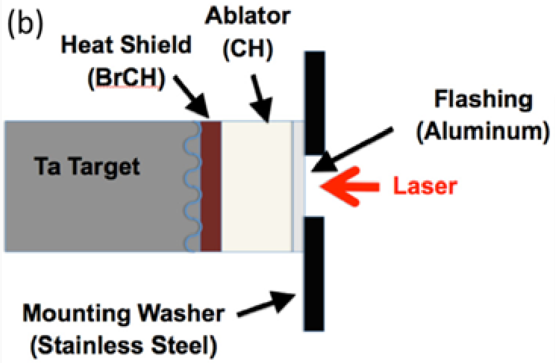

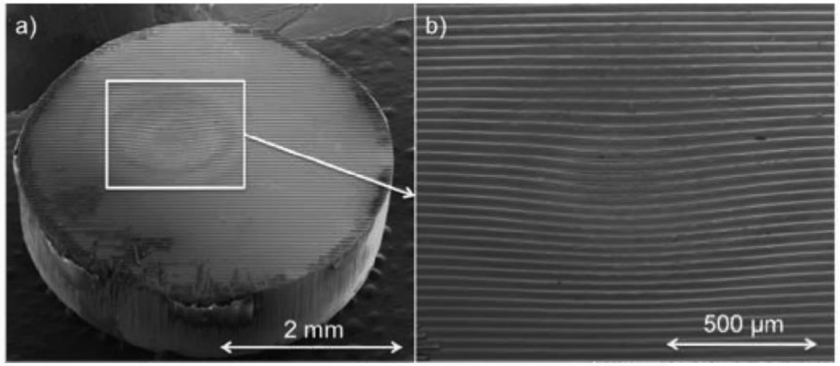

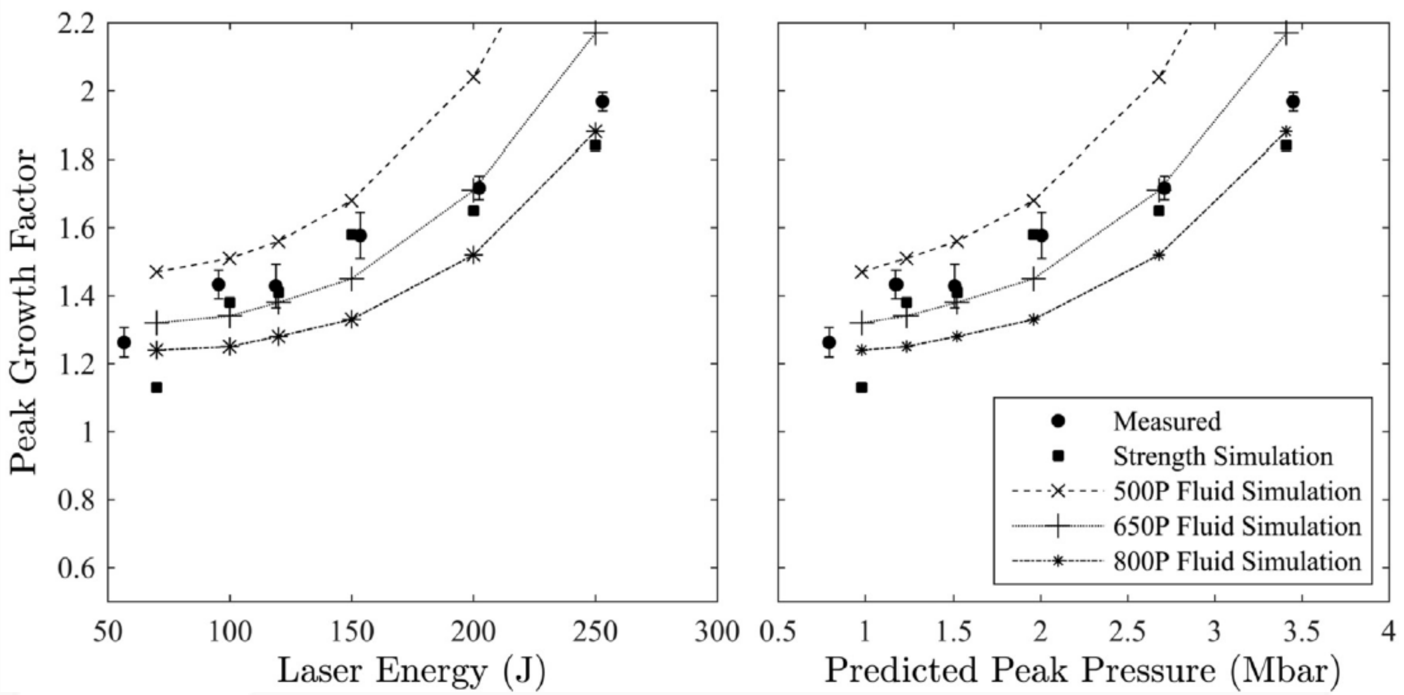

EOS-based model adequately models strength in Mbar regime

A. P. Stebner *et al.*, *Materials Science and Engineering: A*, vol. 732, (2018).

Iron undergoes α-ϵ phase transition when shocked from room temperature.
When shock from higher temperature, it will first transform to γ phase, then ϵ phase.

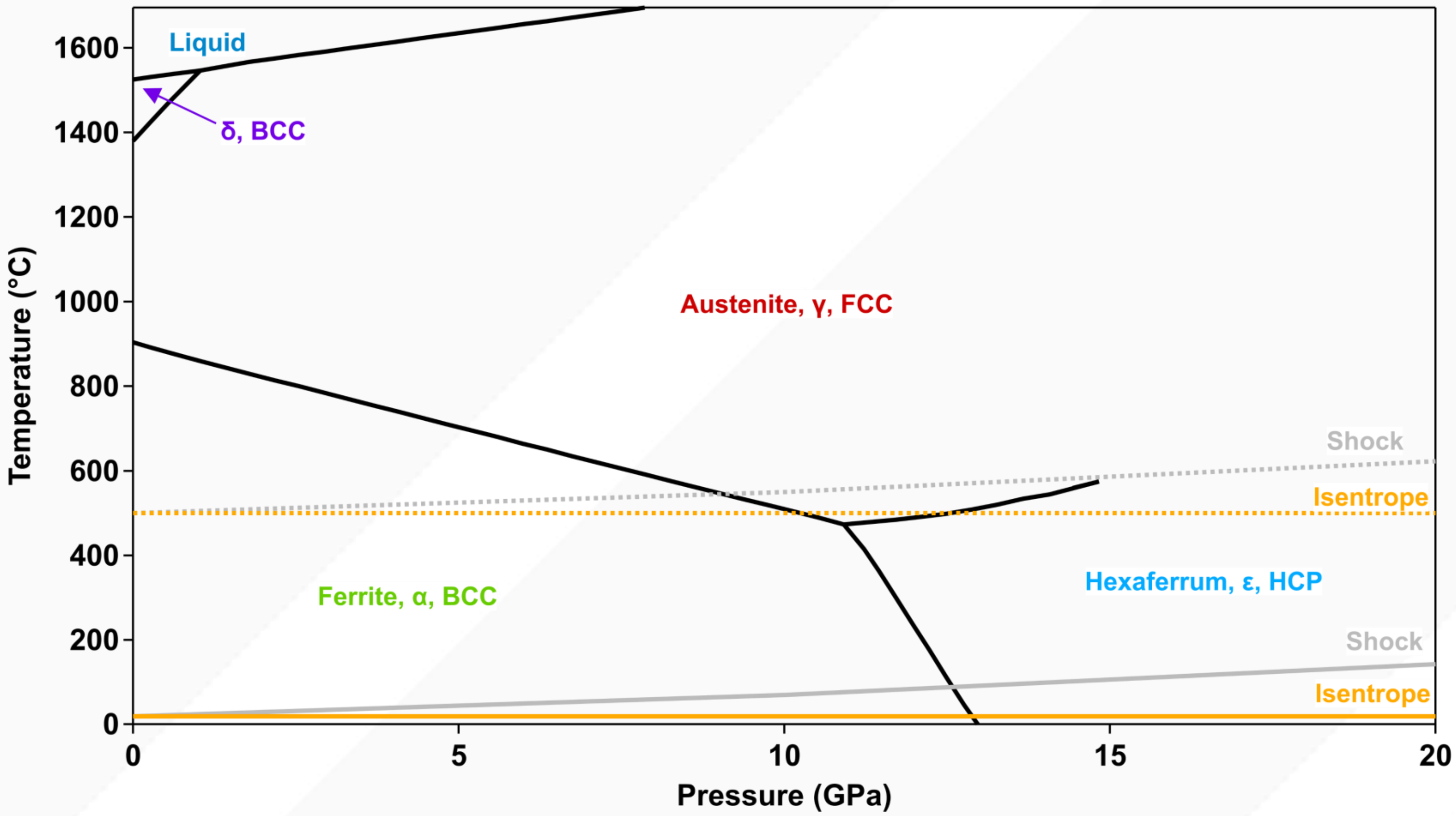

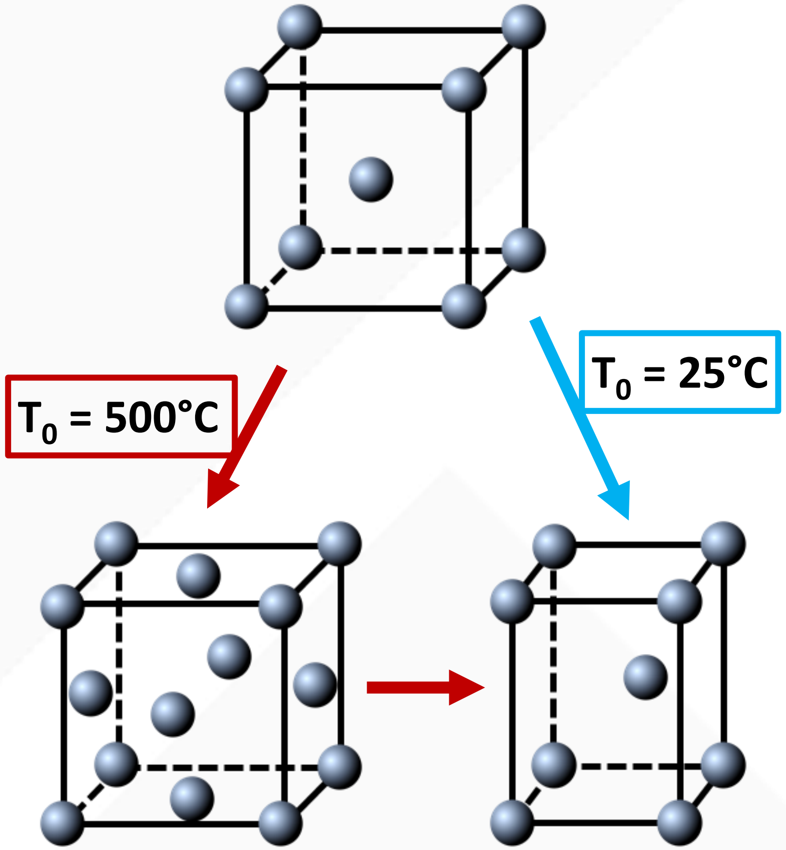

Seismology measurements predict HCP crystals in inner core are anisotropic and aligned along Earth's rotational axis.

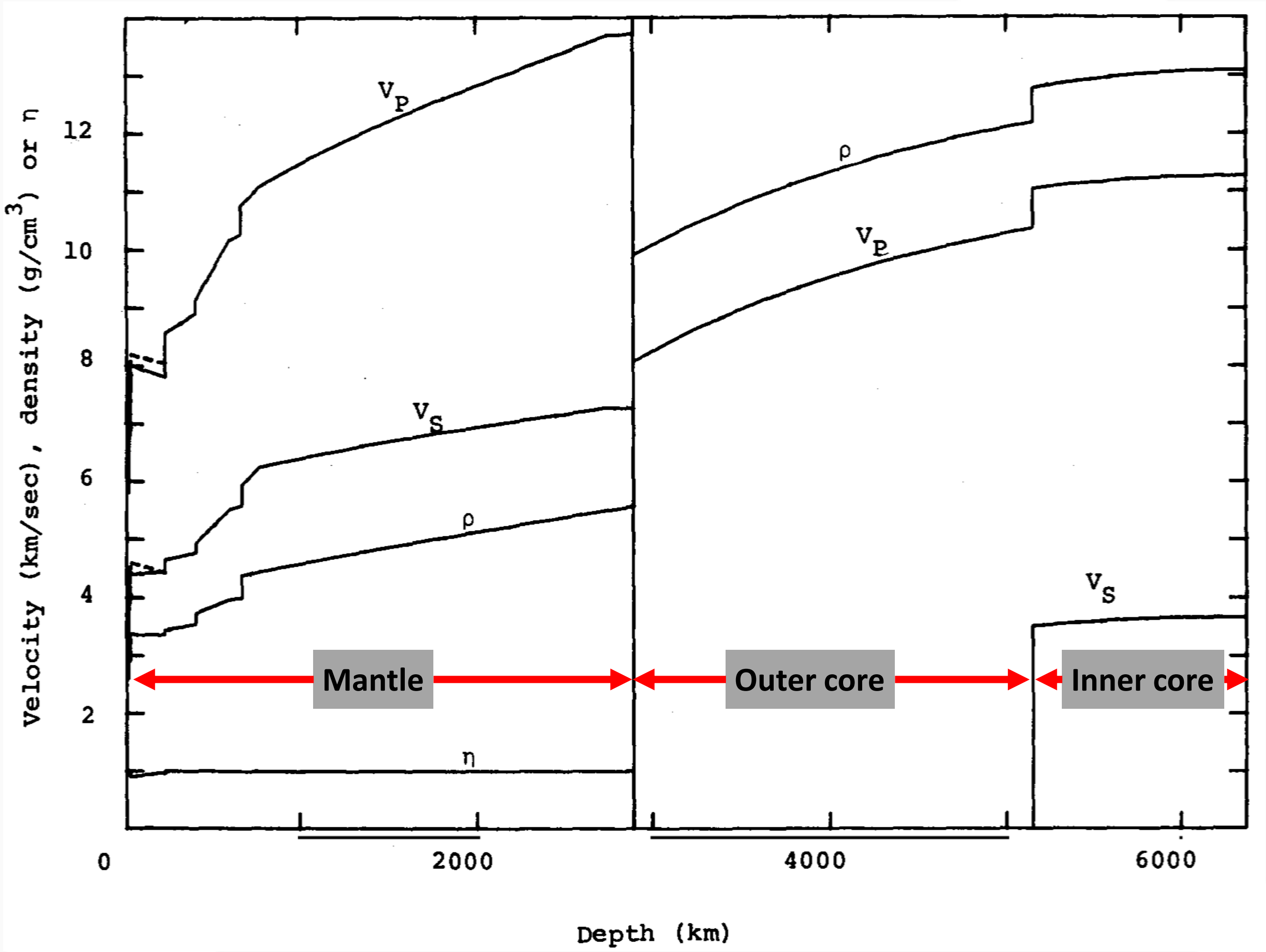

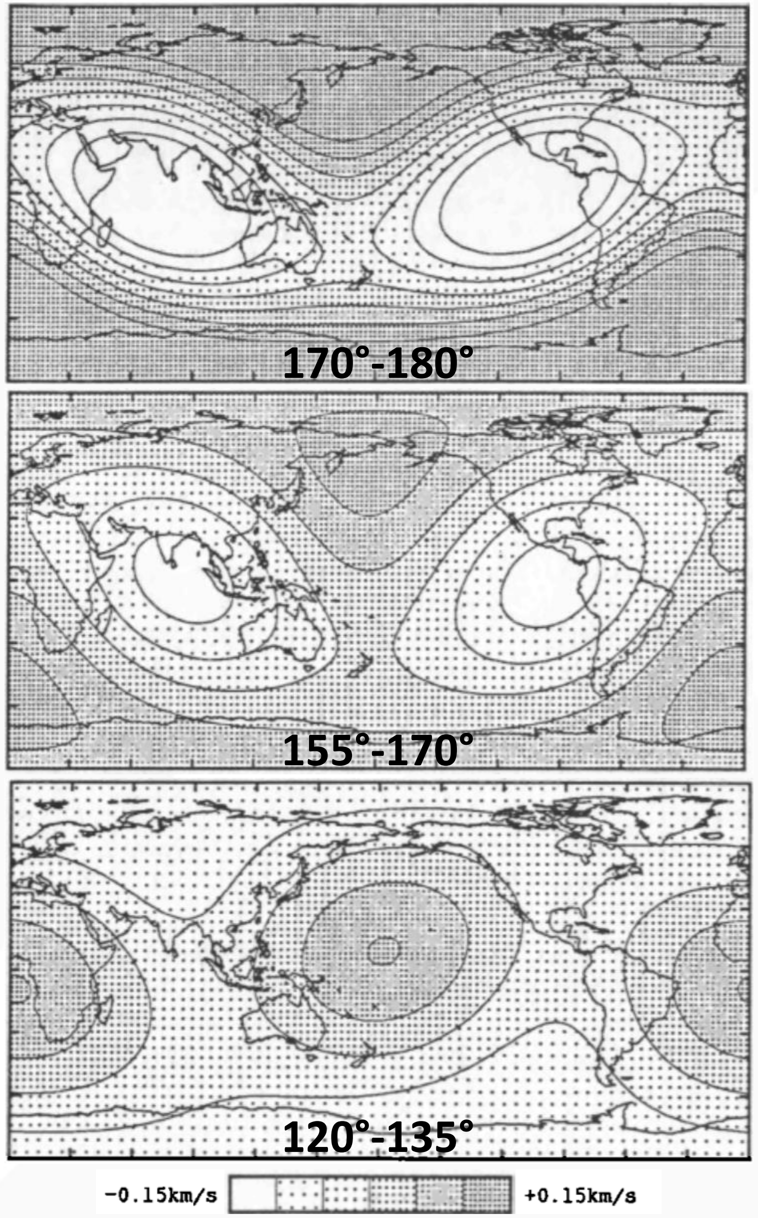

Dziewonski, A.M. and Anderson, D.L. *Phys. of the Earth and Planetary Interiors* 25 (1981)
Morelli, A. et al. *Geophysical Research Letters* 13 (1986).

DAC experiments paired with x-ray probe can be used to measure strength and texture at high pressure.

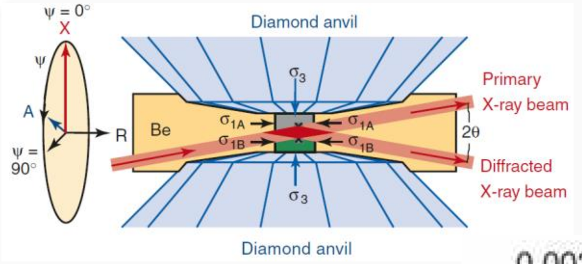

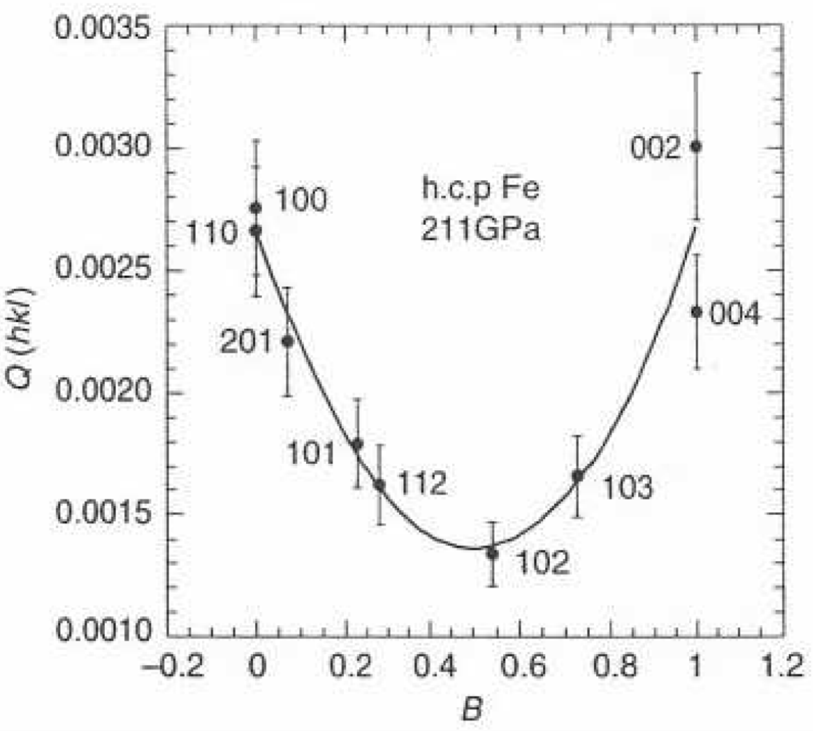

Strong (hkl) dependence of lattice strain reflects a strong elastic anisotropy

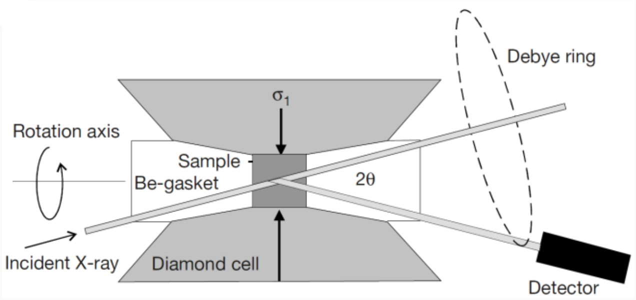

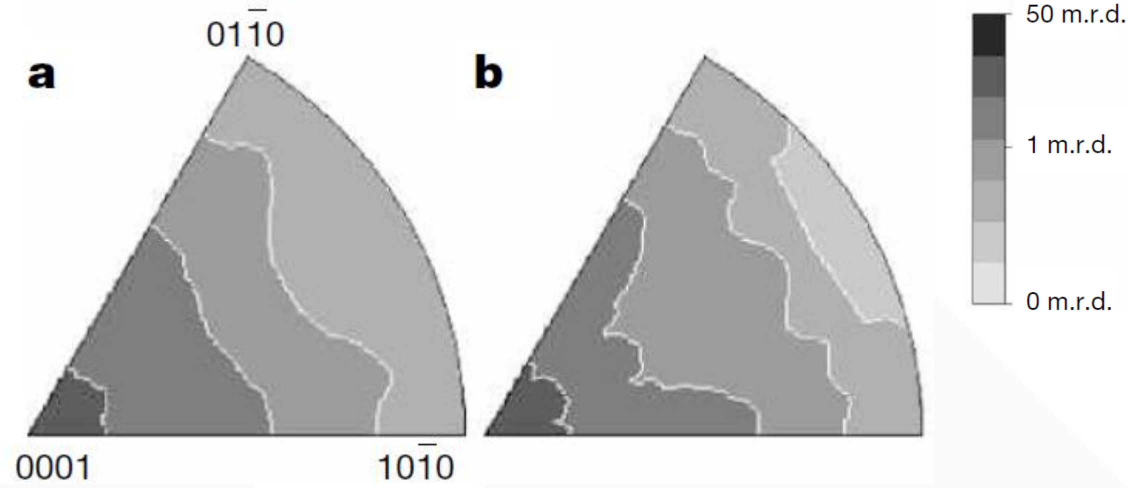

ε-iron crystals display strong preferred orientation

H. Mao, et al., *Nature*, vol. 396, no. 6713, (1998).

H.-R. Wenk, et al., *Nature*, vol. 405, no. 6790, (2000).

DAC experiments paired with x-ray probe can be used to measure strength and texture at high pressure.

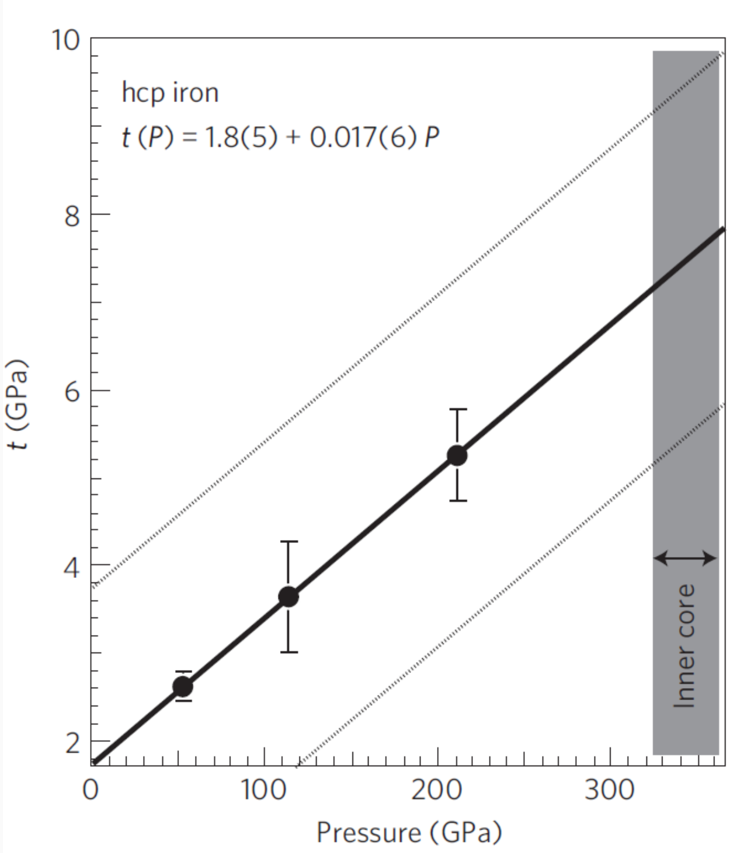

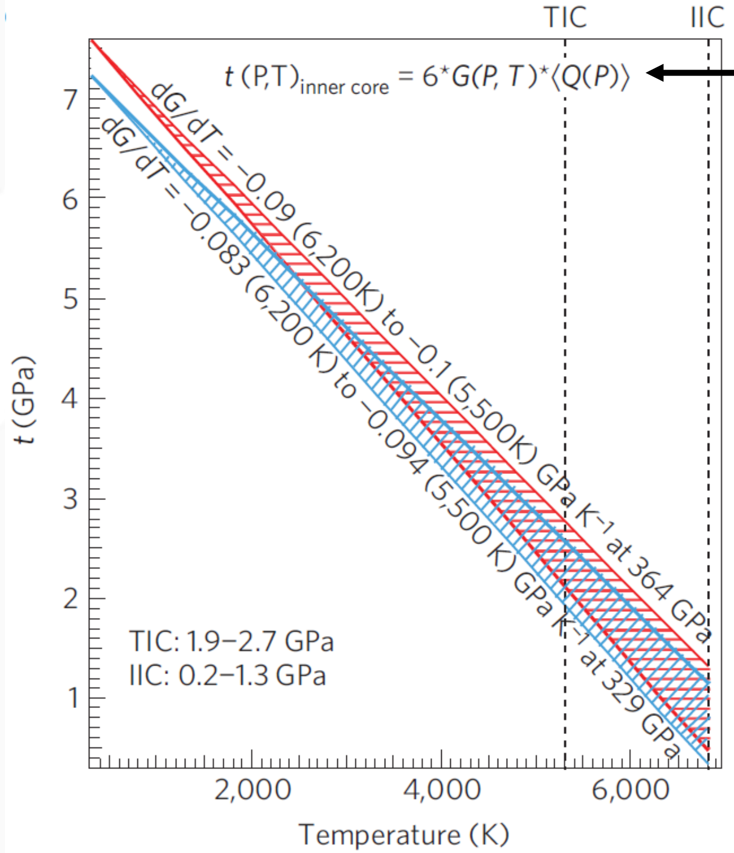

$$\tau(P,T)_{inner\ core} = 6 * G(P,T) * \langle Q(P) \rangle$$

Extrapolated shear stress suggest inner core is weak, supporting creep as dominant deformation mechanism

A. E. Gleason and W. L. Mao, *Nature Geosci*, vol. 6, no. 7, (2013).

High pressure experiments provide additional strength measurements.

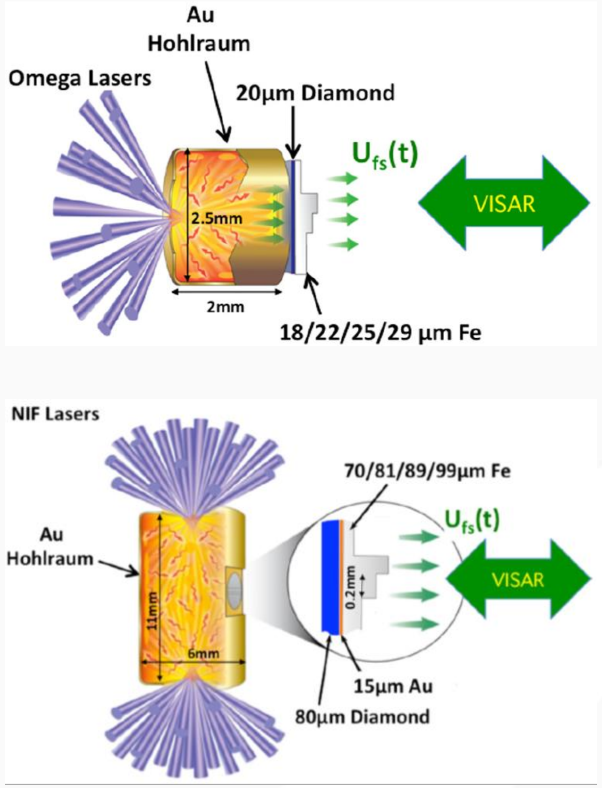

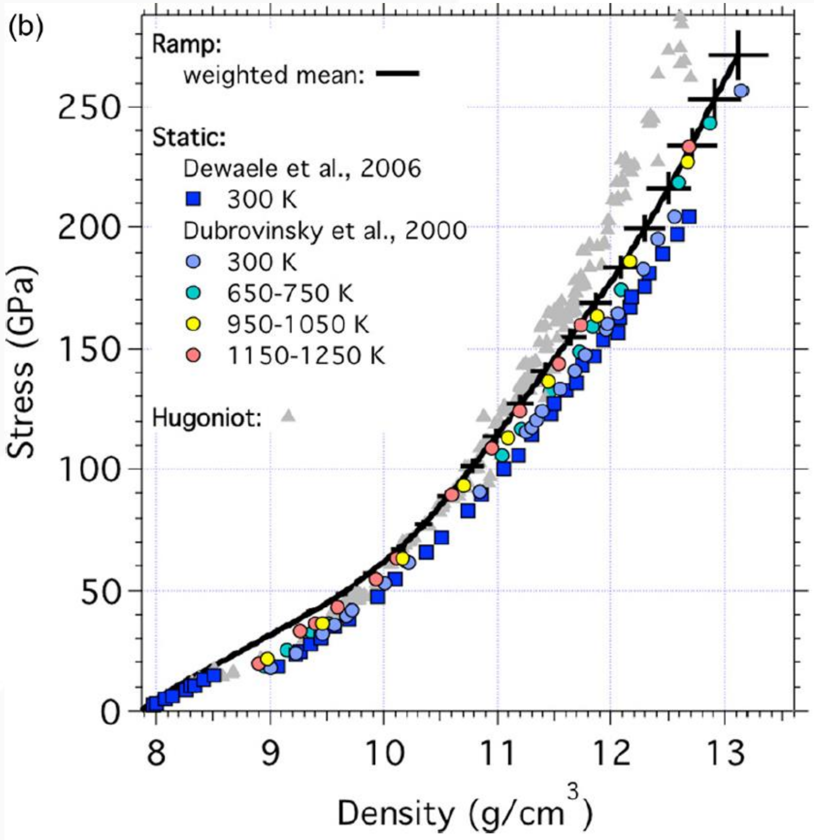

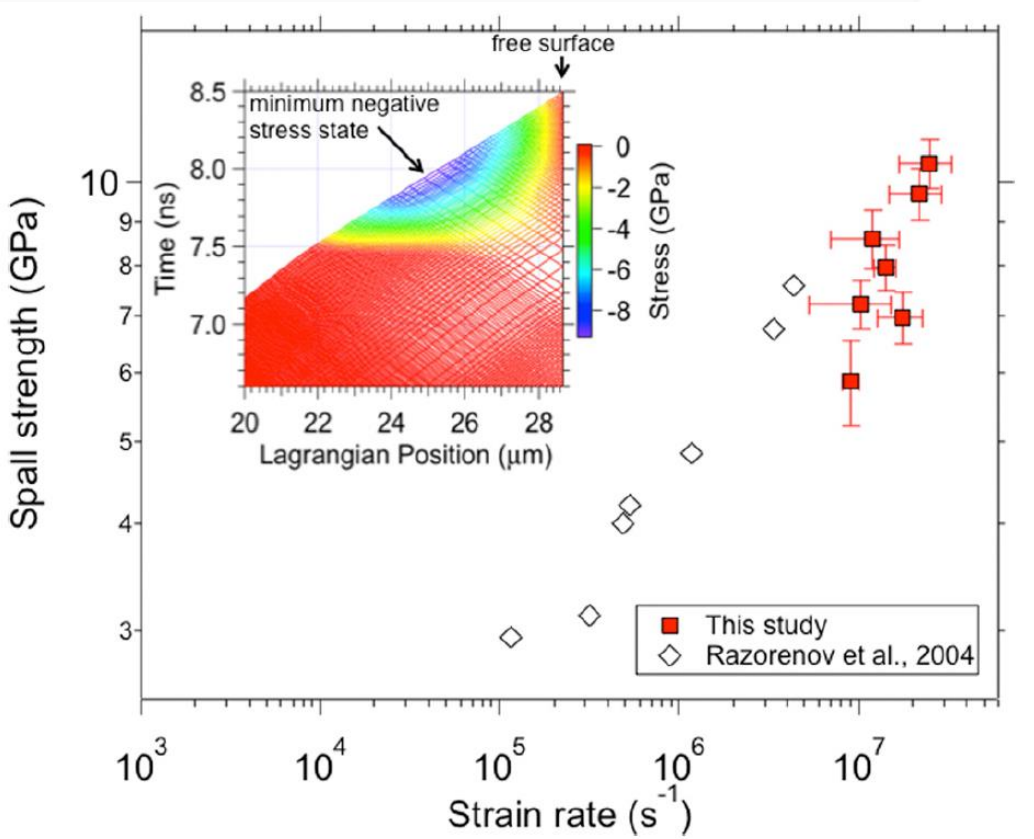

Data is consistent between shock compression and static DAC data

Spall strength increases with increasing strain rate

J. Wang *et al.*, *Journal of Applied Physics*, vol. 114, no. 2, (2013).

Laser shock compression and EXAFS measurements report drastically higher strength at core conditions.

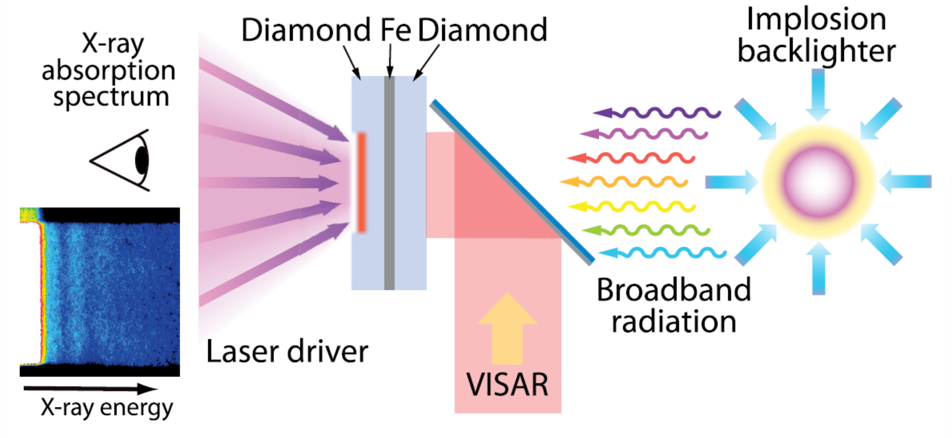

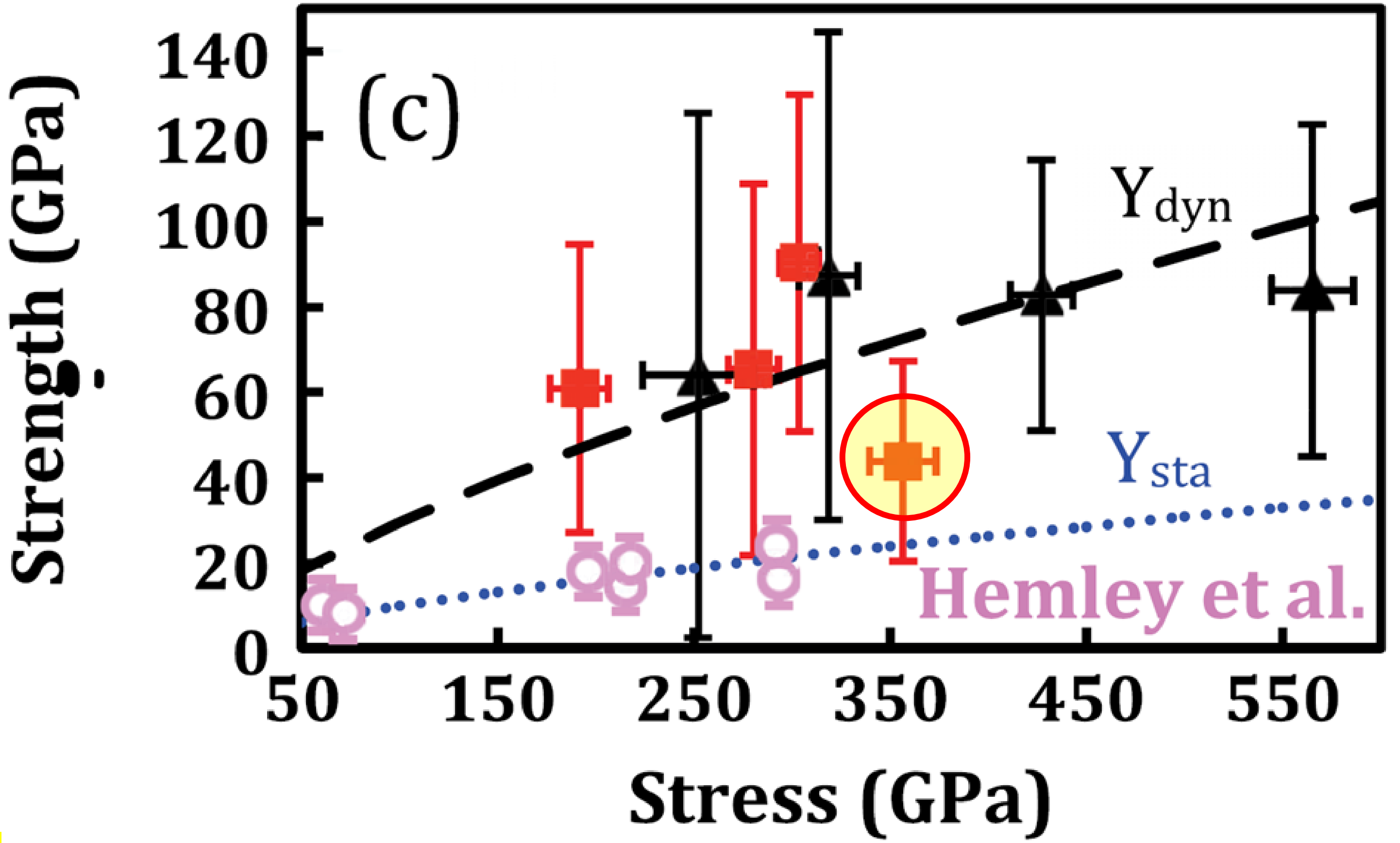

Temperature is higher than expected from pure compression work

Dynamic strength >> static strength

Y. Ping *et al.*, *Phys. Rev. Lett.*, vol. 111, no. 6, (2013).

High pressure experiments provide additional strength measurements.

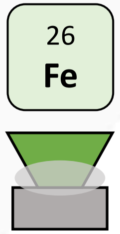

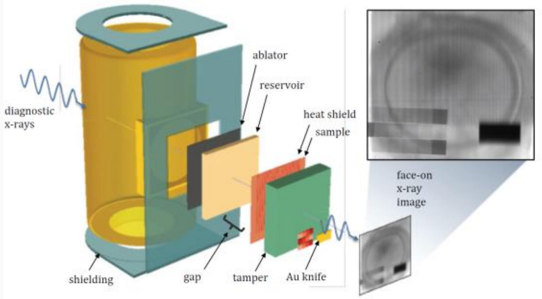

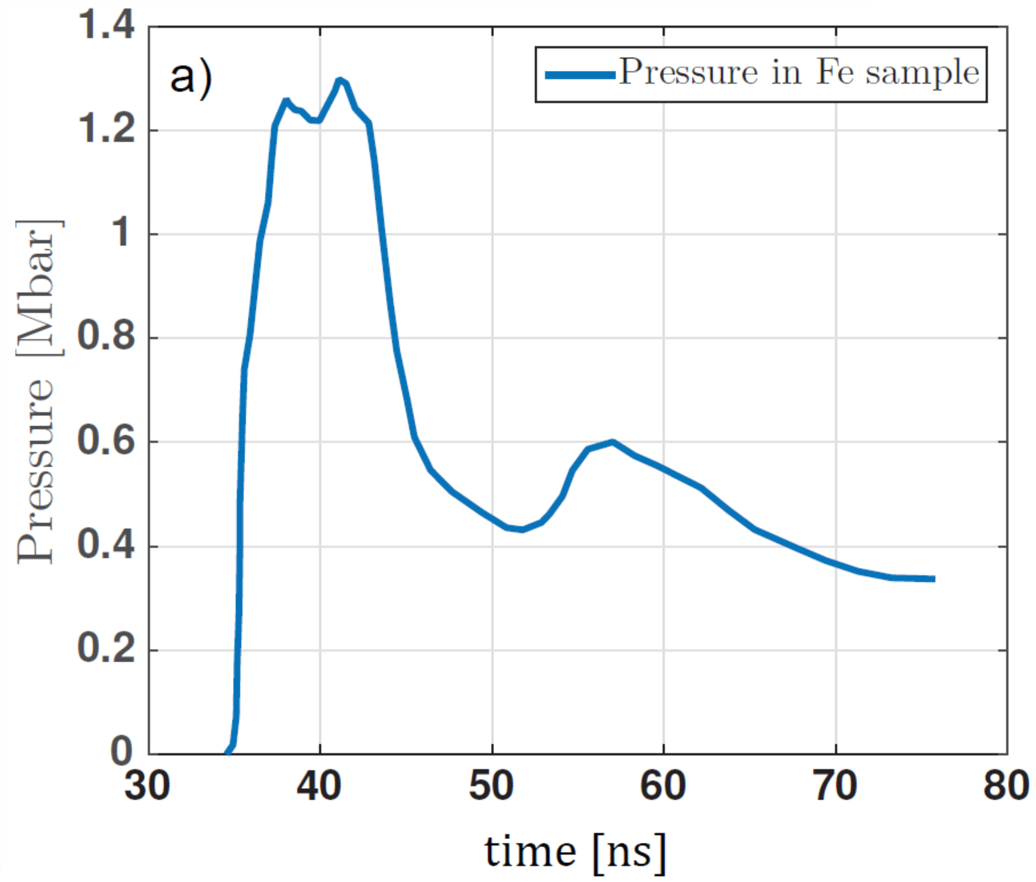

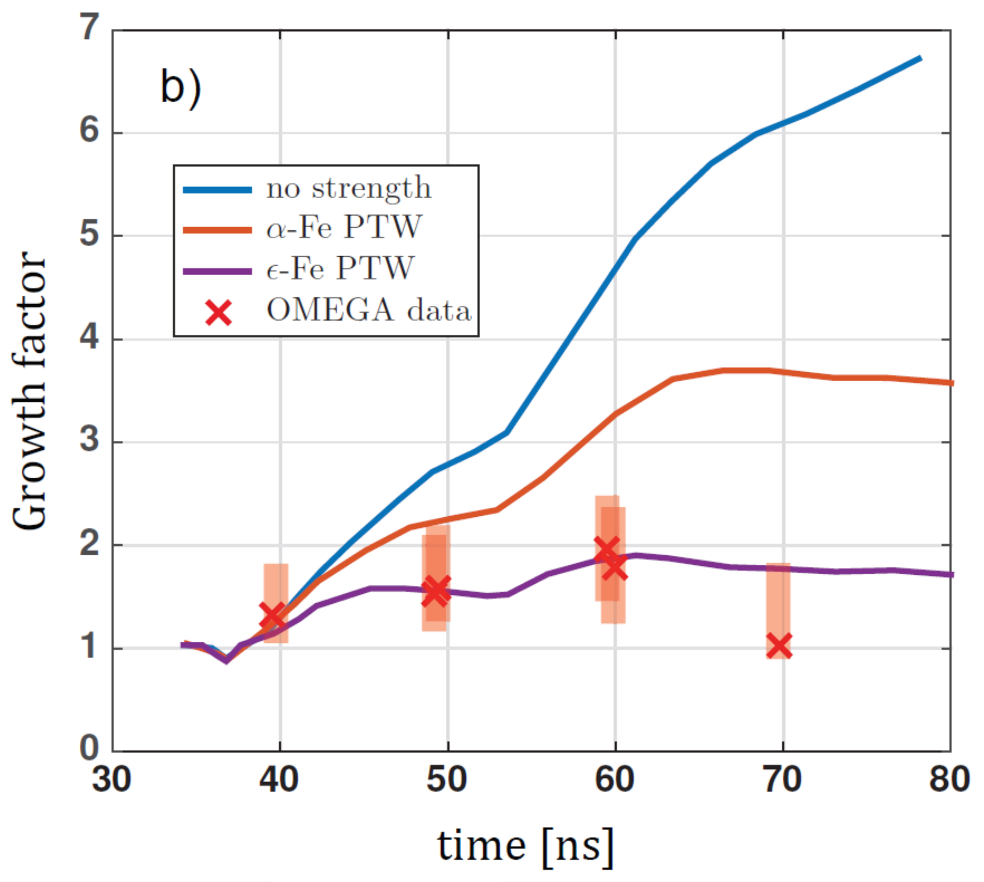

Calculated flow stress > 40 GPa!

C. M. Huntington *et al.*, SHOCK COMPRESSION OF CONDENSED MATTER (2017).

Simulations provide insight into post-shock microstructure and deformation mechanisms.

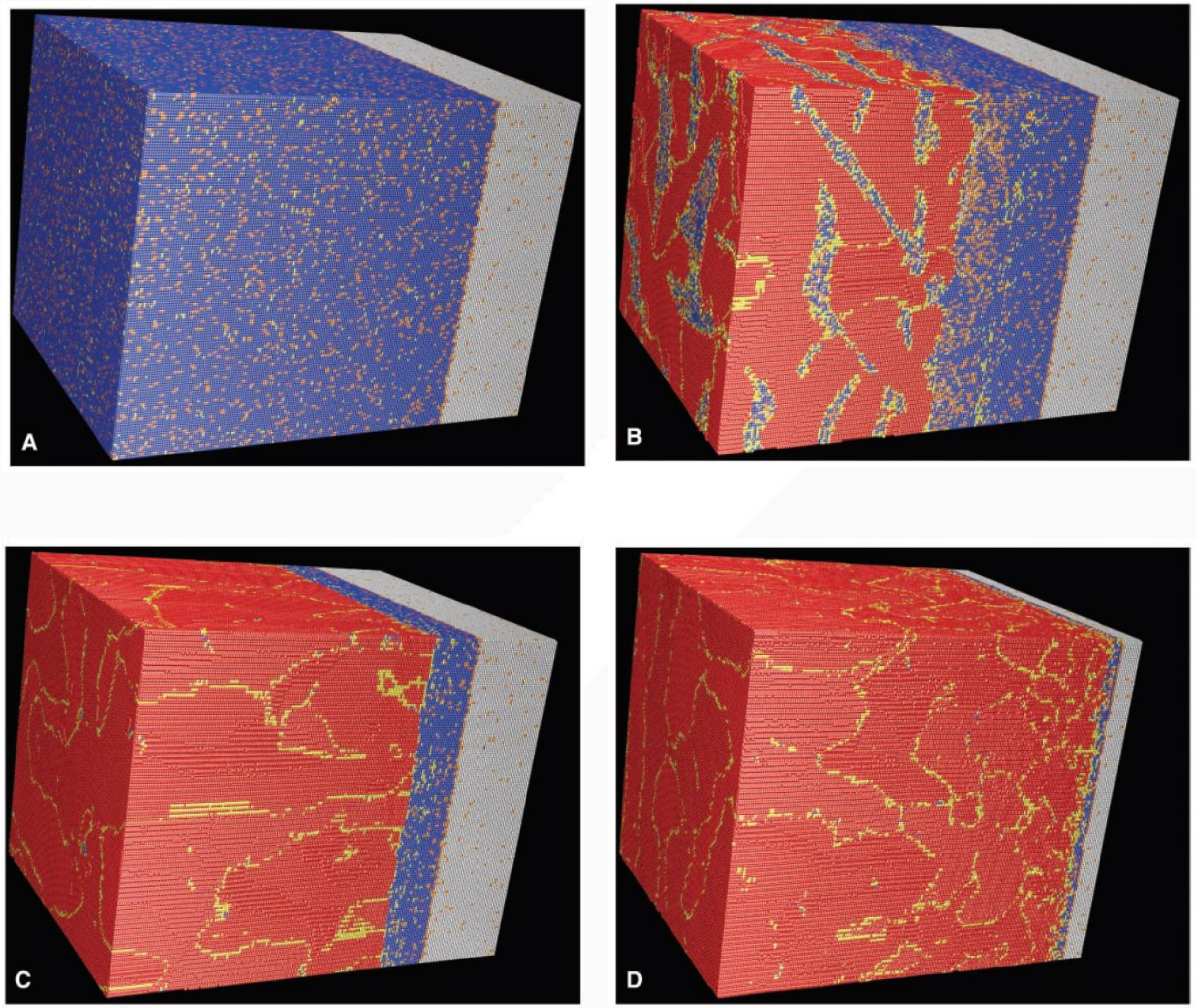

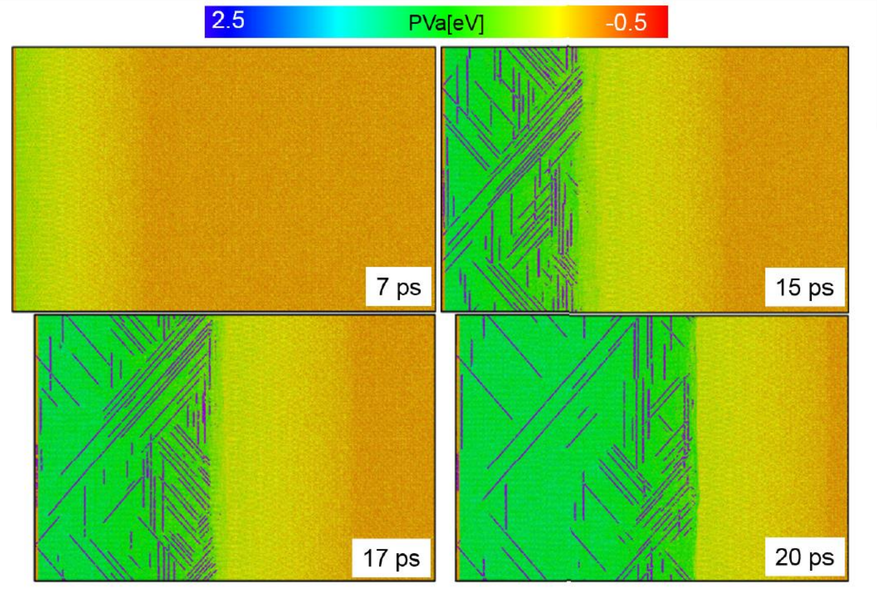

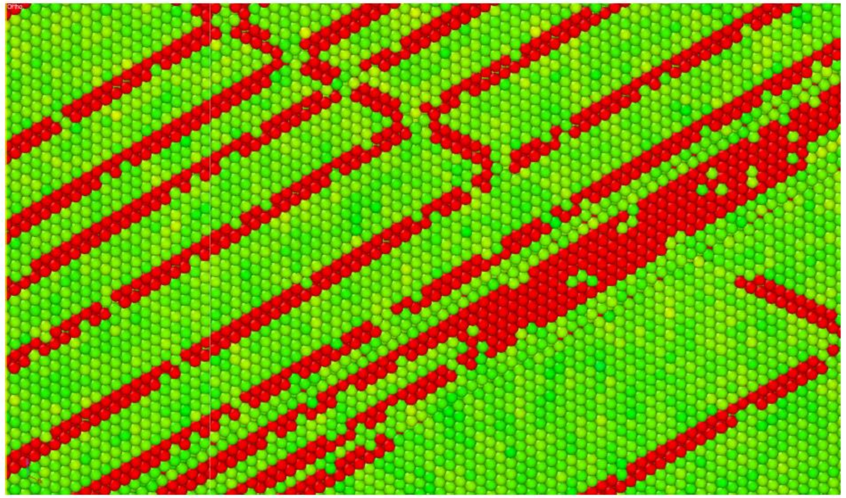

K. Kadau, *Science*, vol. 296, no. 5573, (2002).

N. Amadou, et al., *Phys. Rev. B*, vol. 98, no. 2, (2018).

Summary

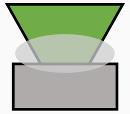

- Extreme conditions are achieved through shock compression, a method to reach ultra-high pressures and strain rates that induce slip and twinning deformation mechanisms.

74 **W**

- Slip and twinning are theorized to cause softening after compressive reloading.

42 **Mo**

- BCC structure remains stable to high pressure under ramp compression or until shock melting.

23 **V**

- High effective lattice viscosity explained by phonon drag mechanism.
- Contradictions to Hall-Petch are found during spallation, follow Grady theory.

73 **Ta**

- Spall strength increases with decreased grain size, following Curran-Seaman-Shockey theory.
- RTI and RMI instabilities measure strength to be drastically higher than ambient value.

26 **Fe**

- High-pressure phase transition affects microstructure and properties in contradicting ways.
  - Strength ranges from 1 GPa – 60 GPa
  - BCC-HCP transition is well characterized through simulations
- Research will focus on effect of high pressure (Earth core-like) conditions.

Future work will include strength measurements in both static and dynamic regimes.

Static and quasi static compression: Instron

Dynamic compression: Hopkinson bar

Shock compression: JLF

Ramp compression: NIF

Low $\dot{\varepsilon}$

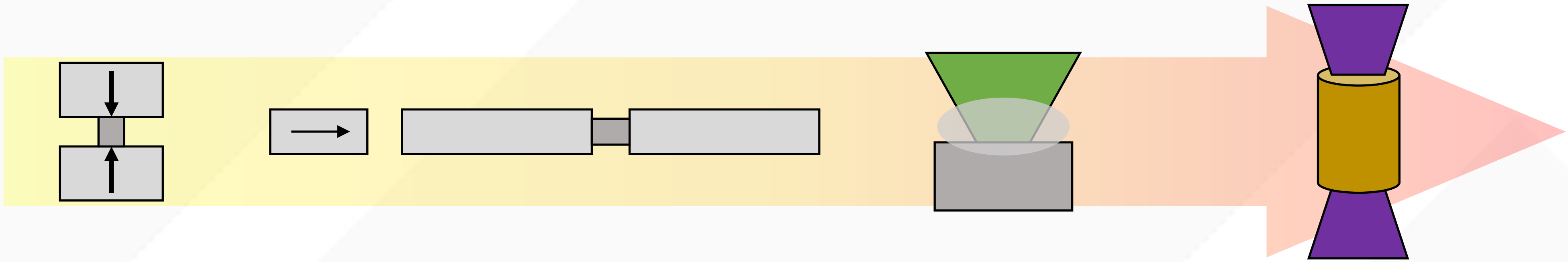

High $\dot{\varepsilon}$

- Experimental:
  - Iron strength dependence on strain rate and grain size
  - Post-shock characterization to analyze defect structure
- Simulations:
  - 1D hydro simulations of spall strength dependence on strain rate

Inner core anisotropy will affect material strength both through stiffness and how the microstructure impedes slip.

26
Fe

Sample	Strength
[001] 6000 K	4 GPa
[111] 6000 K	2 GPa
[001] 2000 K	8 GPa

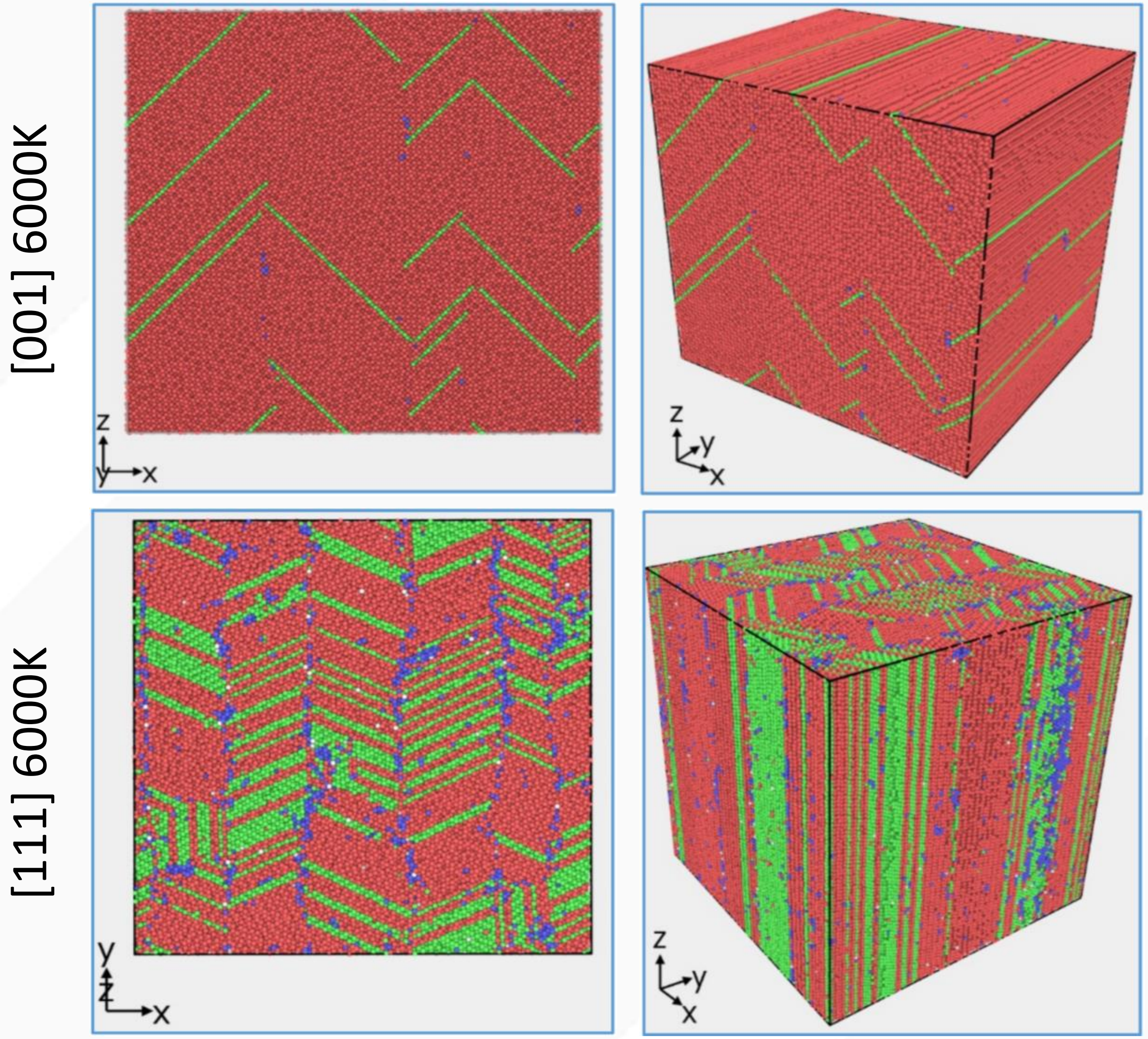

- The same active planes, but grain boundaries appear perpendicular to different axis

Ruestes, Bringa, new results

Acknowledgements

- Committee Members:
  Dr. Marc Meyers, chair
  Dr. Anne Pommier
  Dr. Farhat Beg
  Dr. Nicholas Boechler
  Dr. Javier Garay

- Collaborators:
  Dr. Hye-Sook Park
  Dr. Robert Rudd
  Dr. Arianna Gleason
  Dr. Carlos Ruestes
  Dr. Eduardo Bringa
  Dr. Shiteng Zhao

- This research is funded by:
  Center for Matter Under Extreme Conditions Grant (DE-NA0003842)
  Lawrence Livermore National Lab Academic Collaboration Team grant (subcontract B639114)

CMEC
CENTER FOR MATTER UNDER EXTREME CONDITIONS